DEVELOPMENT OF DAMAGE IDENTIFICATION SCHEME USING DE-NOISED MODAL FREQUENCY RESPONSE FUNCTION DATA WITH ARTIFICIAL NEURAL NETWORK

MOHAMAD IZZUDIN BIN HUSSEIN SHAH

FACULTY OF ENGINEERING
UNIVERSITY OF MALAYA
KUALA LUMPUR

2018

DEVELOPMENT OF DAMAGE IDENTIFICATION SCHEME USING DE-NOISED MODAL FREQUENCY RESPONSE FUNCTION DATA WITH ARTIFICIAL NEURAL NETWORK

MOHAMAD IZZUDIN BIN HUSSEIN SHAH

RESEARCH REPORT SUBMITTED TO THE
FACULTY OF ENGINEERING
UNIVERSITY OF MALAYA, IN PARTIAL
FULFILMENT OF THE REQUIREMENTS FOR
THE DEGREE OF MECHANICAL ENGINEERING

2018

UNIVERSITI MALAYA

ORIGINAL LITERARY WORK DECLARATION

Name of Candidate: MOHAMAD IZZUDIN
BIN HUSSEIN SHAH

Registration/Matric No: KQK 160023

Name of Degree: Master of Engineering

Title of Project Paper/Research Report/Dissertation/Thesis ("this Work"):
Development of Damage Identification Scheme using De-noised Modal Frequency Response Function Data with Artificial Neural Network

Field of Study: Vibration

I do solemnly and sincerely declare that:

(1) I am the sole author/writer of this Work;
(2) This Work is original;
(3) Any use of any work in which copyright exists was done by way of fair dealing and for permitted purposes and any excerpt or extract from, or reference to or reproduction of any copyright work has been disclosed expressly and sufficiently and the title of the Work and its authorship have been acknowledged in this Work;
(4) I do not have any actual knowledge nor do I ought reasonably to know that the making of this work constitutes an infringement of any copyright work;
(5) I hereby assign all and every rights in the copyright to this Work to the University of Malaya ("UM"), who henceforth shall be owner of the copyright in this Work and that any reproduction or use in any form or by any means whatsoever is prohibited without the written consent of UM having been first had and obtained;
(6) I am fully aware that if in the course of making this Work I have infringed any copyright whether intentionally or otherwise, I may be subject to legal action or any other action as may be determined by UM.

Candidate's Signature Date

Subscribed and solemnly declared before,

Witness's Signature Date

Name:

Designation:

Abstract

Damaged identification scheme is used to monitor and locate the damage on a structure. Vibration based damage identification scheme which utilise vibrational modal data is popular due to its non-destructive nature. Past researches used natural frequency, mode shapes and damping ratio for their damage identification scheme. These modal parameters are considered as downstream data which is less sensitive and accurate than upstream data. Frequency Response Function (FRF), the upstream data, is directly measured from the vibration sensors has lesser error produced and high sensitivity. Experimental Modal Analysis (EMA) required the machine or system to be shut down, which lead to high downtime cost. Therefore, by applying Impact-Synchronous Modal Analysis (ISMA), the system does not have to be completely shut down, and yet could obtained EMA comparable vibrational modal data through signal de-noising process. On the other hand, by using the recent technology Artificial Neural Network (ANN), it can make any complex nonlinear input-output relationship by just learning from datasets given to it regardless any discontinuity and without any extra mathematical model. In this study, ANN is used to identify damage and its location on an in-service machine by feeding the de-noised ISMA FRF dataset to train and test the model. Thus, this study will be using the FRF data as the ANN input to identify damage on a running machine. Multilayer Perceptron (MLP) with backpropagation learning algorithm ANN is used in this study. Moreover, this study needs to minimize the number of samples used by reducing number of sensors and frequency range used without affecting the performance accuracy. Finding the relationship between sensor location and the performance accuracy by selecting the correct vibration mode is also one of the objective of this study. The experiment setup is done on a rectangular Perspex plate structure to simulate a structure of a vehicle. EMA and ISMA techniques were used to acquire both datasets, whereby later EMA datasets will be used as a training dataset as for ISMA datasets as the testing datasets. Python language is used in this study and utilized the Keras library with Tensorflow backend. Results shows that this study managed to design a damage identification scheme by using FRF’s datasets with ANN. This study also managed to minimize the number of sensors from nine (9) sensors to a single sensor with a performance accuracy of 100%. Lastly, this study proved that there is a relationship the sensor location and the accuracy of the prediction by selecting the correct vibration mode.

Abstrak

Skim pengenalan kerosakan digunakan untuk memantau dan mencari kerosakan pada struktur. Skim pengenalan kerosakan berasaskan getaran yang menggunakan data modal getaran popular kerana sifatnya yang tidak merosakkan. Penyelidikan yang lalu menggunakan kekerapan semulajadi, bentuk mod dan nisbah redaman untuk skim pengenalan kerosakan mereka. Parameter modal ini dianggap sebagai data hiliran yang kurang sensitif dan tepat daripada data huluan. "Frequency Response Function" (FRF), data huluan, secara langsung diukur dari sensor getaran mempunyai ralat yang lebih rendah yang dihasilkan dan kepekaan yang tinggi. Analisis Modal Eksperimen (EMA) memerlukan mesin atau sistem ditutup, yang mengakibatkan kos downtime yang tinggi. Oleh itu, dengan menggunakan "Impact-Syncronous" Analisis Modal (ISMA), sistem tidak perlu ditutup sepenuhnya, namun dapat memperoleh data modal getaran EMA yang setanding melalui proses de-noising isyarat. Sebaliknya, dengan menggunakan teknologi terkini "Artificial Neural Network" (ANN), ia boleh membuat sebarang perhubungan input-output bukan linear yang kompleks dengan hanya belajar dari dataset yang diberikan kepadanya tanpa mengira apa-apa kekurangan dan tanpa sebarang model matematik tambahan. Dalam kajian ini, ANN digunakan untuk mengenal pasti kerosakan dan lokasinya di dalam mesin dalam perkhidmatan dengan dataset FRF ISMA yang dilancarkan untuk melatih dan menguji model. Oleh itu, kajian ini akan menggunakan data FRF sebagai input ANN untuk mengenal pasti kerosakan pada mesin yang sedang berjalan. "Multilayer Perceptron" (MLP) dengan algoritma pembelajaran "backpropagation" ANN digunakan dalam kajian ini. Tambahan pula, kajian ini perlu meminimumkan bilangan sampel yang digunakan dengan mengurangkan bilangan sensor dan julat frekuensi yang digunakan tanpa menjejaskan ketepatan prestasi. Mencari hubungan antara lokasi sensor dan ketepatan prestasi dengan memilih mod getaran yang betul juga merupakan salah satu objektif kajian ini. Persediaan eksperimen dilakukan pada struktur plat Perspex persegi panjang untuk mensimulasikan struktur sebuah kenderaan. Teknik EMA dan ISMA digunakan untuk memperoleh kedua-dua dataset, di mana kemudian dataset EMA akan digunakan sebagai dataset latihan untuk dataset ISMA sebagai dataset pengujian. Bahasa Python digunakan dalam kajian ini dan menggunakan perpustakaan Keras dengan backend “Tensorflow”. Keputusan menunjukkan bahawa kajian ini berjaya merangka skim pengenalan kerosakan dengan menggunakan dataset FRF dengan ANN. Kajian ini juga dapat mengurangkan bilangan sensor dari sembilan (9) sensor kepada sensor tunggal dengan ketepatan prestasi 100%. Akhir sekali, kajian ini membuktikan bahawa terdapat hubungan lokasi sensor dan ketepatan ramalan dengan memilih mod getaran yang betul.

Acknowledgements

First of all, I wish to express my deepest gratitude to my supervisor Dr. Ong Zhi Chao for offering me to conduct this research project and his exemplary guidance, constant encouragement and monitoring throughout my research project. Every time I came across something that I do not understand, he was always available to advise me and discuss with me in precise details. I learnt a lot about the fundamentals and core knowledge about vibration.

Moreover, I could not do it without the support from my family which helped me acquire my strength to accomplish my project successfully. I am grateful to my friends as well who always stood by me in case of any kind of help I sought for. I would like to express my sincere appreciation to every party that had given support and shared their priceless knowledge with me.

Lastly, I hope that this document will benefit its readers, in providing additional data related to the research of damage detection using frequency response function data for future references and studies.

Table of Contents

List of Figures

List of Figures

List of Tables

List of Symbols and Abbreviations

Abbreviations

ANN	:	Artificial Neural Network
NN	:	Neural Network
MLP	:	Multi-layer Perceptron
BP	:	Backpropagation
EMA	:	Experimental Modal Analysis
OMA	:	Operational Modal Analysis
ISMA	:	Impact-Synchronous Modal Analysis
ISTA	:	Impact-Synchronous Time Averaging
FA	:	Frequency Averaging
SA	:	Spectral Averaging
PCA	:	Principal Component Analysis
APCID	:	Adaptive Phase Control Impact Device
FRF	:	Frequency Response Function
FTF	:	Fast Fourier Transformation
DAQ	:	Data Acquisition
PC	:	Personal Computer
GPU	:	Graphics Processing Unit
UM	:	University of Malaya

Symbols

N	:	Newton

List of Appendices

Chapter 1: Introduction

1.1: Background

Modal analysis is a technique used to determine the inherent dynamic characteristics of a structure which are comprehensively defined by natural frequencies, mode shapes, and damping (Brandt, 2011). It is mainly used in investigating the dynamic behaviour of a mechanical system which provides a better tool for identifying the root cause of vibration problems experience in various engineering fields. Current practice usage of modal parameters from modal analysis have been widely used in structural dynamic modification, sensitivity analysis, force determination, active and passive vibration control, analytical model updating, substructure coupling, structure damage detection, vibration-based structural health monitoring in mechanical, aerospace and civil engineering. Currently two modal analysis techniques being widely used are Experimental Modal Analysis (EMA) (Brown et al., 1979; Allemang & Brown, 1998; Leuridan et al., 1986; Richardson & Formenti, 1982, 1985; Richardson, 1986) and Operational Modal Analysis (OMA) (Brincker et. al, 2000, 2001; Zhang et al., 2001; Jacobsen, 2006). Although, EMA needs the system to be fully shut down in order to acquire the modal parameters so that there is no unaccounted excitation force is induced into the system. 'Artificial' excitation is done on the system by using a measurable impact. As for OMA, it allows analysis to be performed while the system is running but the lack of knowledge of the input excitation forces does affect the extracted model parameters accuracy. OMA is also being used when the structure is too huge to response to the excitation produced in EMA since OMA does not required input excitation of the system. In real situation such as petrochemical plant, the downtime cost is high costing in the range from USD 6,000 to 90,000 per hour (Cheet & Chao, 2016). It is very crucial to find other modal analysis technique that can solve this particular problem. Impact-Synchronous Modal Analysis (ISMA) is a modal analysis technique that able to solve this problem. It can be performed during system operation where there is a presence of ambient forces. ISMA uses Impact-Synchronous Time Averaging (ISTA) before performing the Fast-Fourier Transformation (FFT) to de-noise the unaccounted forces, unlike EMA which uses Frequency Averaging (FA) and Spectral Averaging (SA).

Damage identification scheme is the next step in utilizing the ISMA technique for real-time damage identification at an operating plant. Damage assessment can be considered the most important aspects in evaluating existing structural system at the same time ensuring a safe performance during their service life. Damage identification scheme is used to locate and monitor the damage done on a structure. The stiffness and mass of the structure will change due to the damage, which changes the dynamic response of the system. This is where modal analysis is utilized in damage identification scheme. Though, there are various modal parameters that can be obtained from modal analysis such as Frequency Response Function (FRF), natural frequency, mode shapes and damping ratio that can be used in damage identification scheme. Vibration based damage identification scheme which utilize vibrational modal data is popular due to its non-destructive nature. The vibrational modal data can be divided into two sub-component, upstream data and downstream data. FRF is an upstream data whereby it is directly measured by the vibration sensors, which later undergoes modal extraction algorithm which extracts the downstream data such as natural frequency, mode shapes and damping ratio from the FRF. Upstream data consist of all information of a vibrational modal data, with more sensitivity and lesser error margin. The modal extraction algorithm which extracted the downstream data can further induce errors and less sensitivity (Hakim & Razak, 2014; Gordon & et al., 2017). Therefore in this project, FRF vibration data was used for damage identification scheme.

Utilizing the newly available technology, Artificial Neural Network (ANN), the de-noised FRF data collected using EMA and ISMA technique can be fed into the ANN and use it as a damage identification scheme. ANN mimics a human brain resulting in powerful computational and pattern recognition ability for detecting damage in a structure. The most commonly used ANN in the damage dentification problems are Multi-Layer Perceptron (MLP) (Hakim et al., 2011).

1.2: Problem Statement and Significance of the Research

It is very important to maintain the structure integrity of a machine or system to avoid unexpected downtime. Experimental Modal Analysis (EMA) requires the machine or system to be shut down, which lead to high downtime cost, as for Impact-Synchronous Modal Analysis (ISMA) can be done even when the system is running or during operation. Past research papers mostly used EMA technique to acquire the modal parameters data from the structure which required the structure to be stationary. There are various vibrational modal data that can be used for damage identification scheme and most of past research papers used natural frequency and mode shapes as their ANN's training datasets (Hakim et al., 2006, 2011, 2011a, 2011b, 2013, 2013b, 2014). These modal parameters are considered as downstream data which is less sensitive and accurate than upstream data. FRF, the upstream data, is directly measured from the vibration sensors has lesser error produced and high sensitivity. Therefore, study on damage identification scheme using de-noised (ISMA) FRF data need to be done to produce a robust damage identification scheme of a system during operation. By using state of the art Artificial Neural Network (ANN), it can identify damage and its location on a running machine by feeding the de-noised FRF data into the ANN.

1.3: Objectives of the Research

The objectives of the present research project are: -

- To design a vibration based damage identification scheme using modal Frequency Response Function (FRF) data obtained from EMA and ISMA methods with Artificial Neural Network (ANN).
- To study the performance of the damage identification scheme by reduction of number of training samples in training neural network.
- To study the relationship between the performances of the damage identification scheme and sensor location by the selection of the correct vibration mode within a reduced frequency range.

1.4: Flow of Research

Figure 1.1 shows the flow chart of the project which is based on the objectives. The experiment test impacts were made on a Perspex plate and the accelerometers' responses data which were recorded using the data acquisition system. Multiple time-domain input into the virtual instruments to generate the frequency response functions (FRF) by performing the Fast Fourier Transformation (FFT) operation. Both EMA and ISMA modal analysis methods were done to collect the EMA and ISMA FRF datasets using similar experimental setup. The ANN model parameters tuning was done by adjusting the number of neurons and hidden layers to find the optimized ANN model. The model performance was evaluated using cross-validation method and EMA FRF dataset was used. The optimized ANN model was used to record the output showing how well the model predict and identify the damage and its location. Later, the ISMA FRF dataset was used as the testing datasets on the optimized ANN model (Trained using EMA FRF dataset) to validate the ISMA FRF in order to support the claim of ISMA method produced similar FRF as the EMA with the same experimental setup. Moreover, reducing number of samples used to train the neural network by reducing the number of sensors and frequency range without affecting the performance was the next objective. By using minimal number of sensor, cost and time can be saved. The project also studies the relationship between the sensor location and the performance by selecting the correct vibration mode in reducing the frequency range. Lastly, the final number of sensor and frequency range used that produced the best performance was chosen.

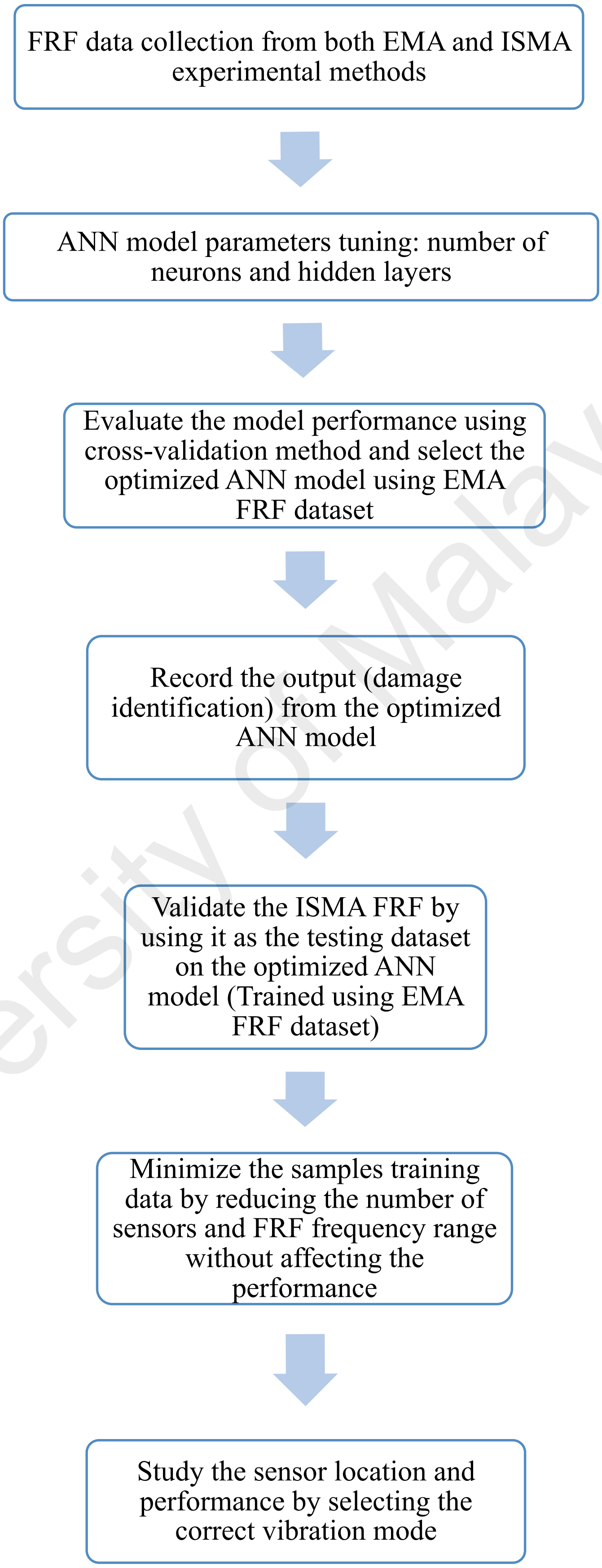

Figure 1.1: Work Flow of the research project

Chapter 2: Literature Review

2.1: Modal Analysis

Modal analysis can be defined as the study of dynamic characteristics of a structure. Dynamic characteristics can be comprehensively define by three main components:-

- Natural frequency
- Mode shapes
- Damping

When an impact is given to a structure, the response is a superimposition of a number of modes and each mode vibrates at its own natural frequency. There are two approaches to undergo modal analysis on a structure, experimental and computational. There are several experimental approaches such as the Experimental Modal Analysis (EMA), Operational Modal Analysis (OMA) and the most recent one called Impact-Synchronous Modal Analysis (ISMA) (Chao, 2013; Rahman et al., 2011, 2013, 2014). Computational modal analysis such as Finite Element also used to generate the model parameters of a structure. Some of the computational software is called ANSYS software which provides wide range of computational not only structural analysis but also fluid flow and heat transfers problem. With these parameters gathered through modal analysis, it can be used to find the root cause of structural problem based on the vibrational modal data. Past studies were done in utilizing both experimental and computational modal analysis data in identifying damage, its location and severity based on the dynamic characteristics (Hakim et al., 2013, 2014). It shows how important the data provided from modal analysis can be utilized with current technology in saving cost and avoid any catastrophic failure of a structure.

2.1.1 Experimental Modal Analysis (EMA)

EMA can be considered the very first modal analysis which is used to study on the vibration characteristics of structure. It involves experimental methods in investigating the oscillation behaviour of component structures. It enables to gather the system's dynamic characteristics, such as natural frequency, mode shape and damping ratio. Structure's mass and stiffness distributions are dependent to the natural frequencies as for the mode shapes are used in structural systems for noise and vibration applications designing. The model parameters extracted from EMA have been widely used in many application, especially in detecting damage on a stationary structure such as beam (Rahman & et al., 2011, 2013, 2014). However, the limitations of traditional EMA is artificial excitation is required to measure the FRFs of the structure. This can be very difficult considering most structures in the field testing are very large in size. Large structures make it harder to response to the excitation produced during EMA. EMA requires the system to completely shut down to avoid any unaccounted excitation force. Measurable impacts are used to produce artificial excitation to excite the system. The responses of the system are auto-corelated and cross-correlated with the measured inputs. Correlation functions are transformed to frequency domain to obtain the transfer function. Moreover, in order to generate the FRFs, Fast Fourier Transformation (FFT) operation needs to be performed. Figure 2.2 shows the FFT function operation which is used in EMA in order to produce the FRF. For forced vibrations of Multiple Degrees of Freedom (MDOF) system with viscous damping, the spatial coordinate equations of motion can be written in matrix form as shown in Eq. (2.1). [M], [C], and [S] are matrices of mass, damping and stiffness respectively. As for $\{\ddot{X}(t)\}$, $\{\dot{X}(t)\}$, $\{X(t)\}$, and {Q(t)] are matrices of accelerations, velocities, displacements and force vectors respectively in the time function. Expanding Eq (2.1) will produce Eq (2.2). An open loop system representing the relationship between input force, output response and dynamic characteristic of a linear system is shown in Figure 2.2.

$$[M]_{nxn}\{\ddot{X}(t)\}_{nx1}+[C]_{nxn}\{\dot{X}(t)\}_{nx1}+[S]_{nxn}\{X(t)\}_{nx1}=\{Q(t)\}_{nx1} \tag{2.1}$$

$$\begin{bmatrix} M_{11} & M_{12} & \cdots & M_{1n} \\ M_{21} & M_{22} & \cdots & M_{2n} \\ \vdots & \vdots & \ddots & \vdots \\ M_{n1} & M_{n2} & \ldots & M_{nn} \end{bmatrix} \begin{Bmatrix} \ddot{X}_1 \\ \ddot{X}_2 \\ \vdots \\ \ddot{X}_n \end{Bmatrix} + \begin{bmatrix} C_{11} & C_{12} & \cdots & C_{1n} \\ C_{21} & C_{22} & \cdots & C_{2n} \\ \vdots & \vdots & \ddots & \vdots \\ C_{n1} & C_{n2} & \ldots & C_{nn} \end{bmatrix} \begin{Bmatrix} \dot{X}_1 \\ \dot{X}_2 \\ \vdots \\ \dot{X}_n \end{Bmatrix} + \begin{bmatrix} S_{11} & S_{12} & \cdots & S_{1n} \\ S_{21} & S_{22} & \cdots & S_{2n} \\ \vdots & \vdots & \ddots & \vdots \\ S_{n1} & S_{n2} & \ldots & S_{nn} \end{bmatrix} \begin{Bmatrix} X_1 \\ X_2 \\ \vdots \\ X_n \end{Bmatrix} = \begin{Bmatrix} Q \\ Q_2 \\ \vdots \\ Q_n \end{Bmatrix} \tag{2.2}$$

The general solution of the linear forced vibration system as shown in Figure 2.2 can be expressed in frequency domain as shown in Equation 2.2, where H(ω) is *n x n* square matrix of FRF which represents the dynamic characteristic of a system. Also, it is a transfer function and names as accelerance. As for $H_1(\omega).Q_1(\omega)$ are *n x 1* frequency varying vectors of accelerations and forces respectively. Expanding Eq. (2.2) will result in Eq. 2.3. Restating Eq. (2.3) in summation form of Eq (2.4). Consider the measurement case where I = 1 and j = 1, Eq. (2.5) is expanded and becomes Eq (2.6). Figure 2.1 shows the contribution from different modes to the FRF. Contribution of mode r to $H_{11}(\omega)$ is given in Eq. (2.7).

$$X(\omega) = H_1(\omega).Q_1(\omega) \tag{2.2}$$

$$\begin{Bmatrix} \ddot{X}_1 \\ \ddot{X}_2 \\ \vdots \\ \ddot{X}_n \end{Bmatrix} = \begin{bmatrix} H_{11} & H_{12} & \cdots & H_{1n} \\ H_{21} & H_{22} & \cdots & H_{2n} \\ \vdots & \vdots & \ddots & \vdots \\ H_{n1} & H_{n2} & \ldots & H_{nn} \end{bmatrix} \begin{Bmatrix} Q_1 \\ Q_2 \\ \vdots \\ Q_n \end{Bmatrix} \tag{2.3}$$

$$\ddot{X}_i = \sum_{j=1}^{n} H_{ij} Q_j \tag{2.4}$$

$$H_{ij}(\omega) = \sum_{r=1}^{n} \frac{\phi_{ir}\phi_{jr}}{-\omega^2 + 2\sigma_r \omega \underline{i} + \omega_{or}^2} \tag{2.5}$$

$$H_{11}(\omega)=\frac{\phi_{11}\phi_{11}}{-\omega^2+2\sigma_1\omega\underline{i}+\omega_{o1}^2}+\frac{\phi_{12}\phi_{12}}{-\omega^2+2\sigma_2\omega\underline{i}+\omega_{o2}^2}+\frac{\phi_{13}\phi_{13}}{-\omega^2+2\sigma_3\omega\underline{i}+\omega_{o3}^2}$$
$$+\frac{\phi_{14}\phi_{14}}{-\omega^2+2\sigma_4\omega\underline{i}+\omega_{o4}^2}\cdots\cdots+\frac{\phi_{1n}\phi_{1n}}{-\omega^2+2\sigma_n\omega\underline{i}+\omega_{on}^2} \tag{2.6}$$

$$H_{11}(\omega)=\frac{\phi_{1r}\phi_{1r}}{-\omega^2+2\sigma_r\omega\underline{i}+\omega_{or}^2} \tag{2.7}$$

For the 1st natural mode, r=1, Eq. (2.7) becomes Eq (2.8) where R is the residual, contributed by other modes. The $H_{11}(\omega)$ obtained is a numerical function made up of a set of discrete values. By selecting a band of frequency around the region of r=1, and curve fitting the FRF using least square method, the mode shape coefficient, the undamped natural frequency and the modal damping can be evaluated.

$$H_{11}(\omega)=\frac{\phi_{11}\phi_{11}}{-\omega^2+2\sigma_1\omega\underline{i}+\omega_{o1}^2}+R \tag{2.8}$$

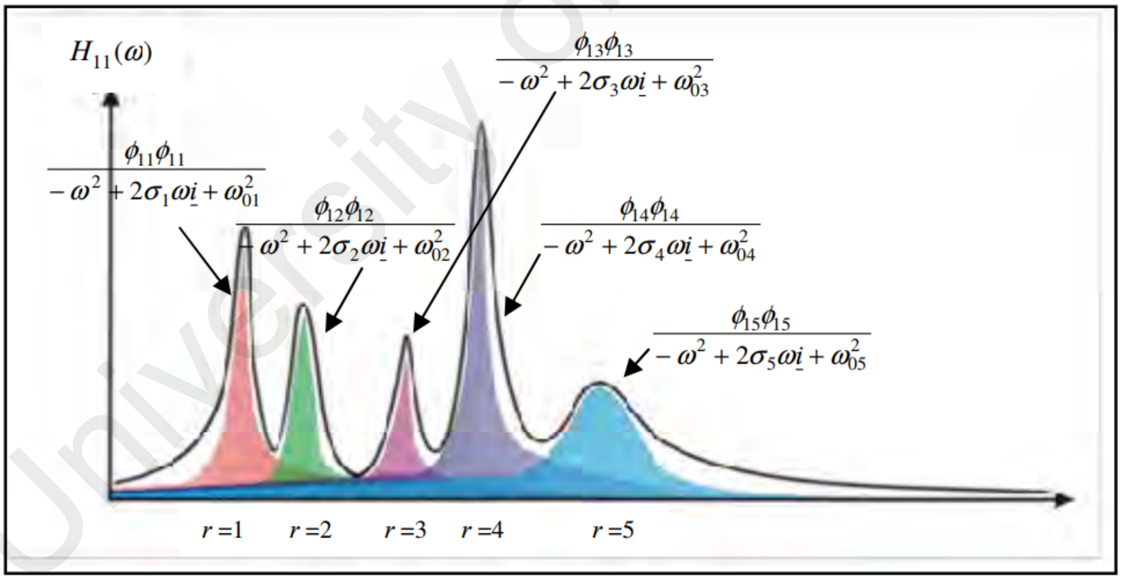

Figure 2.1: Contribution of Natural Modes (Chao, 2013)

In condition where EMA is carried out while the machine is in operation, *X(ω)*, will be the linear superimposition of all the forces induces as shown in Equation (2.9). This includes the artificial excitations, Q_1, from the measured impact force input along with other unaccounted operating forces Q_2, Q_3, Q_4 and so forth. It can be seen transfer function $H_1(\omega)$ is from the measured force input and transfer and transfer function H_2, H_3 and so forth are due to other unaccounted operating forces.

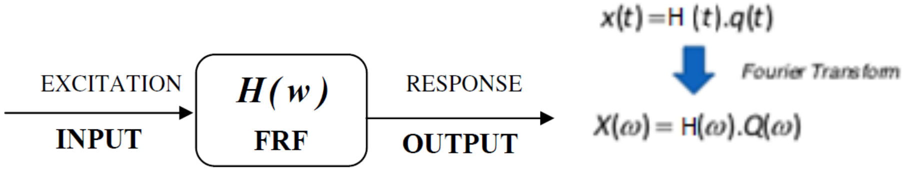

Figure 2.2: FFT function used in EMA in order to produce the FRF

$$X(\omega) = H_1(\omega).Q_1(\omega) + H_2(\omega).Q_2(\omega) + H_3(\omega).Q_3(\omega)+\ldots \qquad (2.9)$$

EMA used Frequency Averaging (FA) and Spectral Averaging (SA) prior to performing FFT, adopting frequency domain averaging. The noise produced by a rotating machine is unpredictable, which can alter the spectrum's shape and lead to serious distortion towards the spectrum. In FA, a series of spectra are averaged together in order for the noise to gradually assume a smooth shape. As for SA, it is commonly used in industrial application of EMA, whereby block averaging is performed in frequency domain. The real and imaginary components of the transfer function are averaged separately.

2.1.2 Operational Modal Analysis (OMA)

There are several past research on Operational Modal Analysis (also known as ambient modal identification) whereby the system can avoid a complete shutdown. It has its own advantages over EMA in terms of user-friendly and practicality in carrying out the procedure. It does not required input excitation to the system unlike in EMA. Therefore, the excitation used is generated by their own operation of the structure. OMA is consider using output (O/O) data. OMA with output-only measurements can be utilised not only for structural control, but also in-situ vibration based health monitoring and damage identification of the structures (Whelan et al., 2011). OMA can be performed when the system is running in order to measure the vibrational responds. However, OMA procedures are limited to cases where excitation to the system is white stationary noise.

The challenges encountered in the OMA are that the noise-to-signal ratio in the measured data is much higher than in the controlled experiment in laboratory environment and output-only data can only be used for parameter identification. Also, the modal parameters that are gathered do get affected with the lack of information on the input excitation forces. The mode shapes processed from this technique did not able to normalize accurately, leading to affect the mathematical models. Figure 2.3 shows the ambient responds system whereby the inputs are assumed to have Gaussian amplitude distribution.

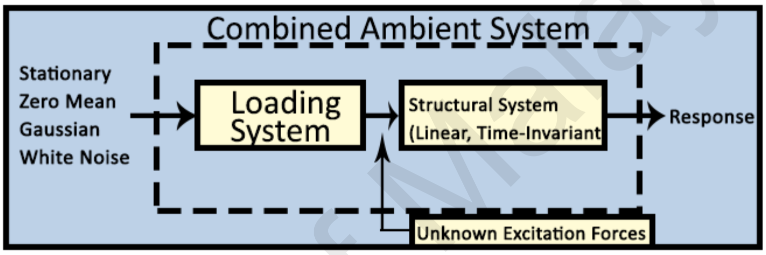

Figure 2.3: Combined ambient model

There are many techniques used to extract the modal parameters from output-only data (Dion and et al., 2012; Lardies & Larbi; 2001a). Balanced Realization (BR) and Canonical Variate Analysis (CVA) were the two correlation-driven stochastic subspace algorithms. BR can do multiple measurements with similar excitation which can be globally modelled in one model. As for CVA requires an individual analysis of each measurement. CVA might result in discrepancies for the frequency and damping estimates of the same mode for the different measurements. Also, BR identifies the modal parameters in one step. Therefore, computational load of the BR method is significantly better.

Moreover, past research paper presented a modal parameter identification method which takes the harmonic excitations into account while performing OMA (Mohanty & Rixen, 2004). The technique is based on the Ibrahim Time Domain (ITD) method and explicitly includes the harmonic frequencies called Single Input Multiple Output (SIMO) Single

Station Time Domain (SSTD) (Zaghlool, 1980). With this, it allows proper identification of eigenfrequencies and modal damping even when harmonic excitation frequencies are close to the natural frequency of the structures.

2.1.3 Impact Synchronous Modal Analysis (ISMA)

ISMA is integrated with Impact-Synchronous Time Averaging (ISTA) which allows analysis to be performed in the presence of ambient forces (Chao, 2013; Rahman et al., 2011, 2013, 2014). ISMA can be considered better than OMA in terms of performing modal analysis on a in-service or running machine. As shown in Equation (2.9), the non-synchronous component is filtered out in the time domain by ISTA, leaving only the responses triggered due to the impact hammer as shown in Equation (2.10). ISTA is utilized prior to performing the FFT operation to acquire the FRF. In time domain synchronous averaging, signal acquisition from rotating machine is triggered at the same rotational position of the shaft using a tachometer for every cycle. The time block of the averaged signal eliminates all the non-synchronous and random components, leaving behind only components that are integer multiples of the running speed. In ISMA, the same and simple averaging concept is used but only to achieve the reverse i.e. to filter out all the speed synchronous and random signatures. In this case, data acquisition is triggered by the impact signature. The periodic signatures and their harmonics are no more in the same phase position for every time block acquired. Averaging process will slowly diminish these non-synchronous components hence leaving behind only the structure's response to impulses which are synchronous to the repetitive impact force. Cross spectrum of the averaged time block of impulse responses and the averaged time block of impact signatures is used to generate the transfer function. It is worthwhile to note that responses from unaccounted forces that contain even the same frequency as that contained in the impulse response, is diminished if the phase is not consistent with the impact signature.

$$X(\omega) = H_1(\omega).Q_1(\omega) \quad (2.10)$$

Past research paper compared between ISTA technique in ISMA with FA and SA techniques used in EMA (Chao, 2013). Results showed that FA merely smoothens the spectrum, while ISTA and SA produce similar quality of the Transfer Functions. Also, further improvement on the ISMA was done in the research paper by conducting a study on the effect of the important parameters in ISMA such as number of averages, impact frequency, exponential window and amount of impact force applied. The number of averages and impact frequency are important parameters when performing ISMA on structures which are in operations.

The modal parameters extraction follows similar procedures as the EMA. High accuracy modal parameters extracted from the analysis performed during operation with the information of input forces in the transfer functions. ISMA has been successfully used in both rotor and structural dynamic systems to determine the modal parameters of systems without interrupting the operations (Rahman et al., 2011, 2013, 2014). The Adaptive Phase Control impact Device (APCID) is the main device which eliminates non-synchronous components in order to produce minimal possible impacts applied by feeding the phase angle information (Cheet & Chao, 2016). It is proven that APCID can improve the effectiveness of ISTA in FRF estimation and reduce time required in performing modal analysis. Lastly, previous research study of phase synchronization effect is done in the post processing stage showed that the number of averages can be greatly reduced, thus fasten the overall analysis procedure if the phase angle of the disturbance with respect to the impact is found (Chao et al., 2015, 2016).

2.2: Damage Identification Scheme

Damage in a machine or structure usually leads to failure. Damage in a structure is defined as reduction in mass and stiffness of the structure that can affect the functionality and safety, which finally can lead to structural failure. Therefore, it is important to monitor the structure integrity if there is any damage occurrence. The modal parameters such as the FRF, mode shapes, damping ratio and natural frequencies will change when damage happens in a structure. There are four (4) levels of damage identification as shown in Figure 2.4 (Rytter, 1993).

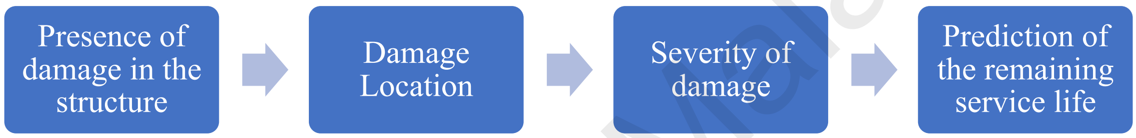

Figure 2.4: Levels of damage identification

The fourth level, remaining service life, usually related with the structure fatigue life and fracture mechanics. Damage identification scheme is important in order to reduce the maintenance costs, increase serviceability and most importantly increase safety of the structures. In this study, the scope will only cover until the second level which is the damage location on the structure. There are many methods used for damage identification scheme from previous research papers. The two commonly reliable approaches are by using the ANN and principal component analysis. Principal component analysis is a method used for feature extraction. The idea is to reduce a large number of measured data to a much smaller number of uncorrelated variables while retaining as much as possible of the variation in the original data.

2.2.1 Modal Parameters used in Damage Identification Scheme

Vibration based damage identification scheme which utilize vibrational modal data is popular due to its non-destructive nature. The vibrational modal data can be divided into two sub-component, upstream data and downstream data. FRF is an upstream data whereby it is directly measured by the vibration sensors, which later undergoes modal extraction algorithm which extracts the downstream data such as natural frequency, mode shapes and damping ratio from the FRF. The natural frequency, mode shapes and damping ratio are extracted from the FRFs during data processing phase using ME'Scope software. Upstream data consist of all information of a vibrational modal data, with more sensitivity and lesser error margin. The modal extraction algorithm which extracted the downstream data can further induce errors and less sensitivity (Hakim & Razak, 2014; Gordon & et al., 2017). In the field of civil engineering, most past studies used the natural frequency and mode shape (downstream data) as their ANN training datasets for their damage identification scheme in a structure (Hakim et al., 2006, 2011, 2011a, 2011b, 2013, 2013b, 2014). Studies that used natural frequency as the inputs for their ANN found that a changed in dynamic properties of a structure caused shifts in natural frequency. This frequency shifts managed to indicate a damage occurred on the structure itself due to change of dynamic properties. Another approach is by using the mode shapes, which was found to be more sensitive to damage than natural frequency (Park & et al., 2009). Previous studies managed to produce a robust identification scheme by using only the natural frequency, mode shape and some even uses the damping ratio. They ran an EMA on a non-operating structure such as cantilever beam and bridge girder. In order to avoid the error margin produced during data processing phase, FRF vibration data was used in this research project for damage identification scheme.

2.3: Overview of Artificial Neural Networks (ANN)

Artificial Neural Network is a main Machine Learning (subset of Artificial Intelligence) tool which mimics the biological neuron of animal brains. It is widely used in both industrial and academia world, since recently the existence of deep learning (subset of Machine Learning) where it adds multiple layers into the neural network (deep-neural network) making it more robust and advanced. Nowadays, the abundant amount of data are left untouched and this is where neural network comes in to bring beneficial result from the data itself. ANNs follow the similar brain process, where they learn from given input and output values making it a data-driven modelling technique. Depending on how complex the data is, the neural network will be more effective when high amount of data is fed into the ANN. Figure 2.5 shows how two different techniques scale with amount of data used to train the tool. Most common applications of ANN are stock market prediction, pattern recognition, face recognition, audio recognition, and even used in translating and reading text language (Natural-Language Processing). The reasons why many researchers are interested in applying ANN technique rather than using old techniques such as parameters study, optimization and statistical method are because:-

- Gives higher accuracy
- Simple methodology
- Can solve complex problems
- Universal approximation capability
- Learn based on the data and trying to find the correlation in both supervised and unsupervised approach.

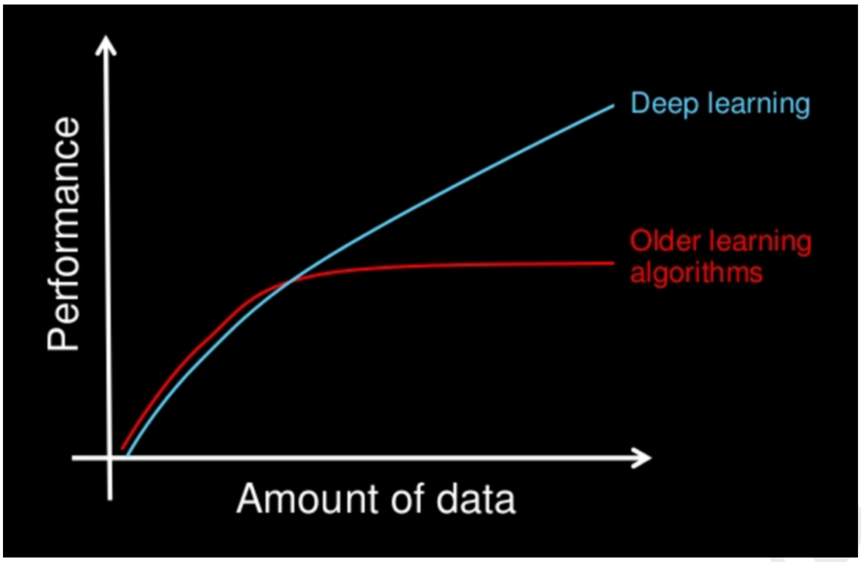

Figure 2.5: The performance of the two different techniques scale with amount of data used to train the tool

2.3.1 Artificial Neuron

The word neuron itself represents a nerve cell in a brain where the function is to receive, process and transmit information as shown in Figure 2.6. The artificial neuron does the same thing as the biological's except the input and the output is in form of numerical values.

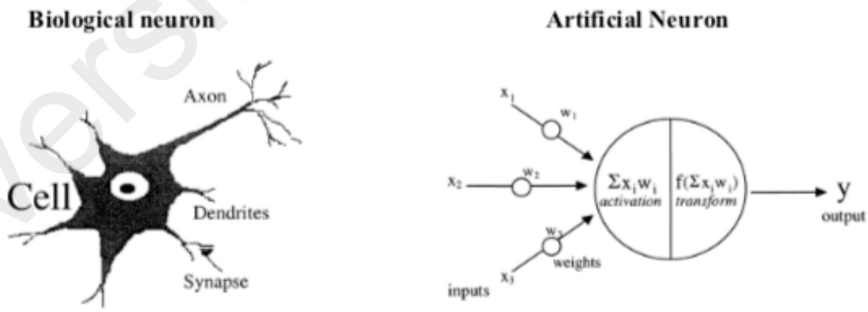

Figure 2.6: Identical concept between biological and artificial neuron

The artificial neuron consists of four (4) main elements:-

- Input
- Net function
- Transfer Function: Activation function used to define the output based on the set of inputs.
- Output

The net function and transfer function are the mathematical model of the artificial node in producing the output based on the input as shown in Equation (2.11). The input will be multiplied by synaptic weights (net function) before proceed to the transfer function. The synaptic weights are just a random values which define the strength of individual input that connects to a node. Weights are the most critical element in ANN due to the weights adjustment is done based on the ANN learning process. Lastly, the resultant value of the net function will proceed to the transfer function producing an output value. Figure 2.7 shows the basic structure of the node7

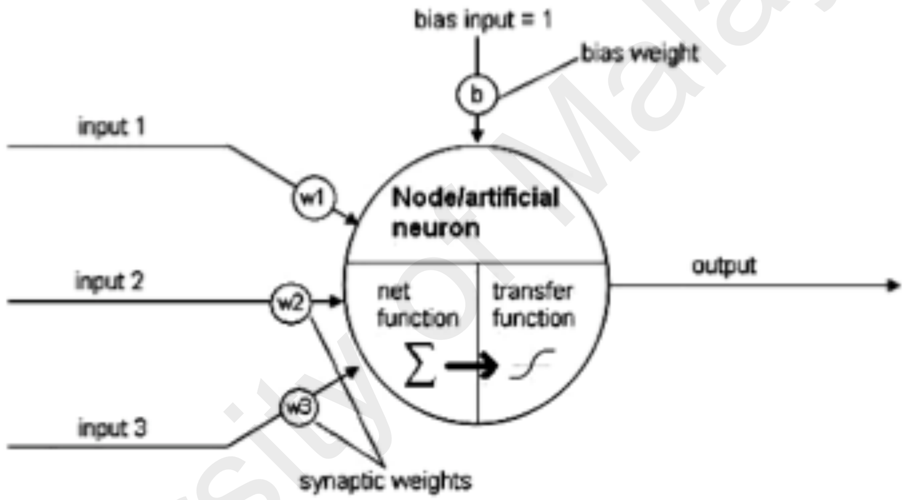

Figure 2.7: Artificial neuron/Node basic structure

The net function can be expressed as:

$$u = b + \sum_{j=1}^{N} w_j \, x_j \tag{2.11}$$

u: output

N: number of inputs

x: input

w: weights

b: bias weights

2.3.2 Artificial Neural Network (ANN)

There are several ways to improve the performance of the ANN model. It can be improve with data, algorithms, algorithm tuning and ensembles (How To Improve Deep Learning Performance, 2016). One of the ways to improve performance with data is by getting more amount of data as stated earlier in the overview. It is important to understand what it means by number of data. Data can be defined as the sample input used in the ANN relative to the outputs. The more number of inputs feed into the ANN for each output, the higher the performance of the ANN. In this study, the amount of data can be improved by adding more number of averages for each output, not adding more sensor or frequency range. The other approaches to improve performance with data are by inventing, rescaling, transforming the data and feature selection. Also the performance of the ANN model can be improved with algorithms. The approaches are by spot-checking algorithm, citation from previous literature review and resampling methods. The third method to improve the performance of the ANN model is with algorithm tuning consists of diagnostics, weight initialization, learning rate, activation functions, network topology, batches and epochs, regularization, optimization and loss and early stopping. In this study, the activation functions, network topology (number of hidden layers and neurons) and batches and epochs were done to improve the performance of the ANN model. The fourth method to improve the performance will by using ensembles. Ensembles can be done through combining different ANN models together whereby each model performs well on the problem and combine their prediction by taking the mean.

Furthermore, there are several types of neural network and learning algorithm that can be used when designing a neural networks model. Figure 2.8 shows a complete list of all types of neural network that can be found (Veen, 2016). The most basic neural network will be the Perceptron (P). Depends on the type and complexity of the problem, different neural network is specified in solving different types of problem. For example, Long/Short Term Memory neural network is specialized in solving a time series prediction problem. Most past research uses the most basic Feed Forward and Radial Basis Network (RBN) for damage identification scheme using modal analysis (LeClerc, 2007; Worden et al., 2000; Hakim et al., 2013, 2013b, 2014). Multi-Layer Perceptron (MLP) is a class of feedforward network which consist of at least 3 layers and uses the backpropagation as the learning algorithm. Backpropagation is used to compute the gradient of the cost function. The ANN can learn their weight and biases from the well-known gradient descent algorithm. In this study, the ANN model need to solve a classification problem, whereby the model needs to predict whether the structure is damaged or undamaged along with the damage location based on the conditions created. Therefore, MLP is the most simple and robust methods to solve ANN classification problems.

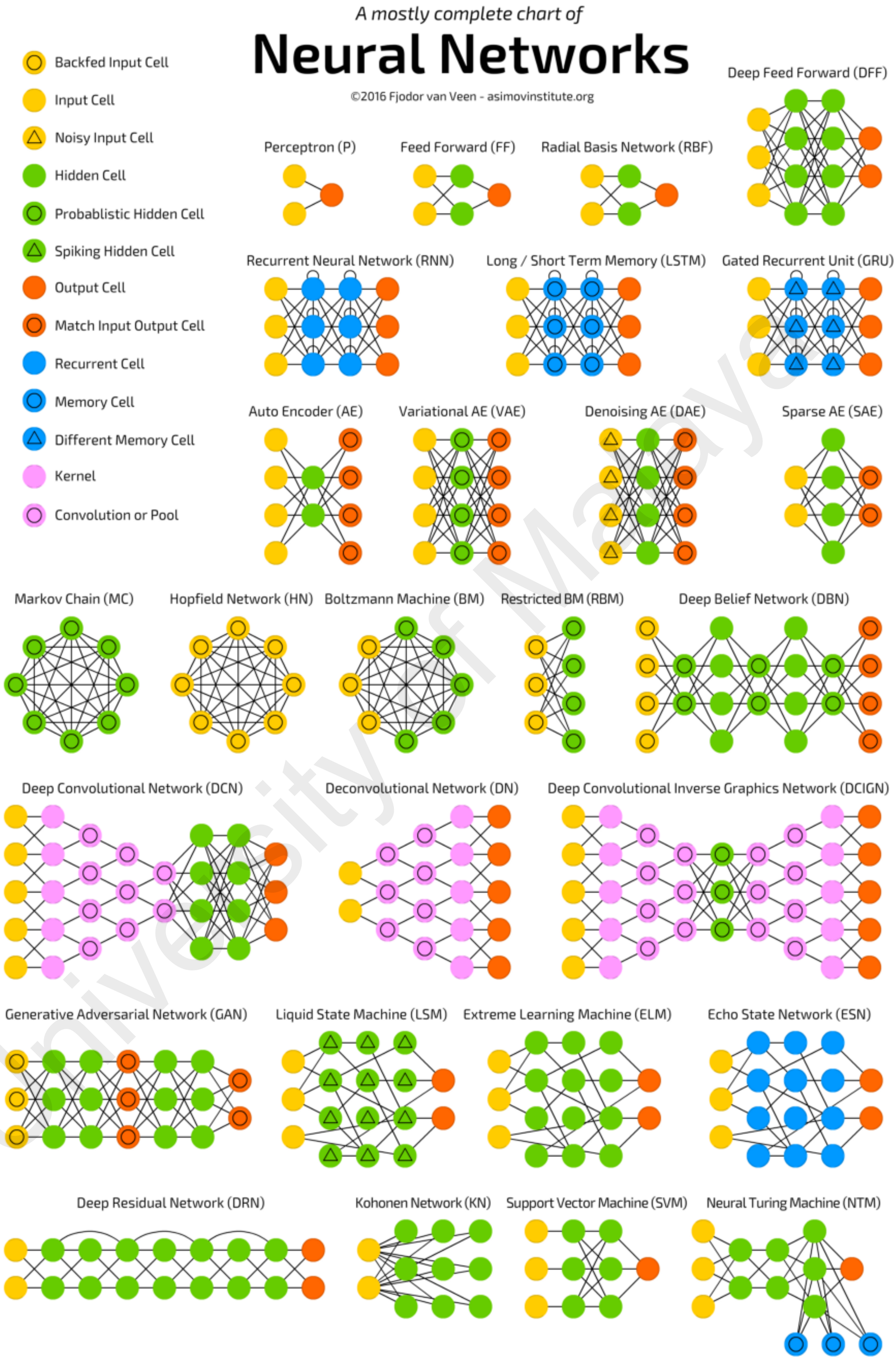

Figure 2.8: Complete chart of ANN taken from (Veen, 2016)

Chapter 3: Methodology

3.1: Equipment and Experimental Set-Up

A rectangular Perspex plate with a dimension of 48cm x 20cm x 0.9cm (width x height x thickness), weighting 1.1kg, was taken as the test specimen as shown in Figure 3.1. In order to simulate a similar vibration behaviour of a car, a rectangular plate was taken as the testing specimen. A car structure can be simplified into a plain structure which consist of a few DOF (Weaver et al., 1990). In this experiment, the test rig was able to represent the small structural model of a car body since car motion includes transitional and rotational modes about the mass centroid of its structure, where it commonly appears in low frequency area.

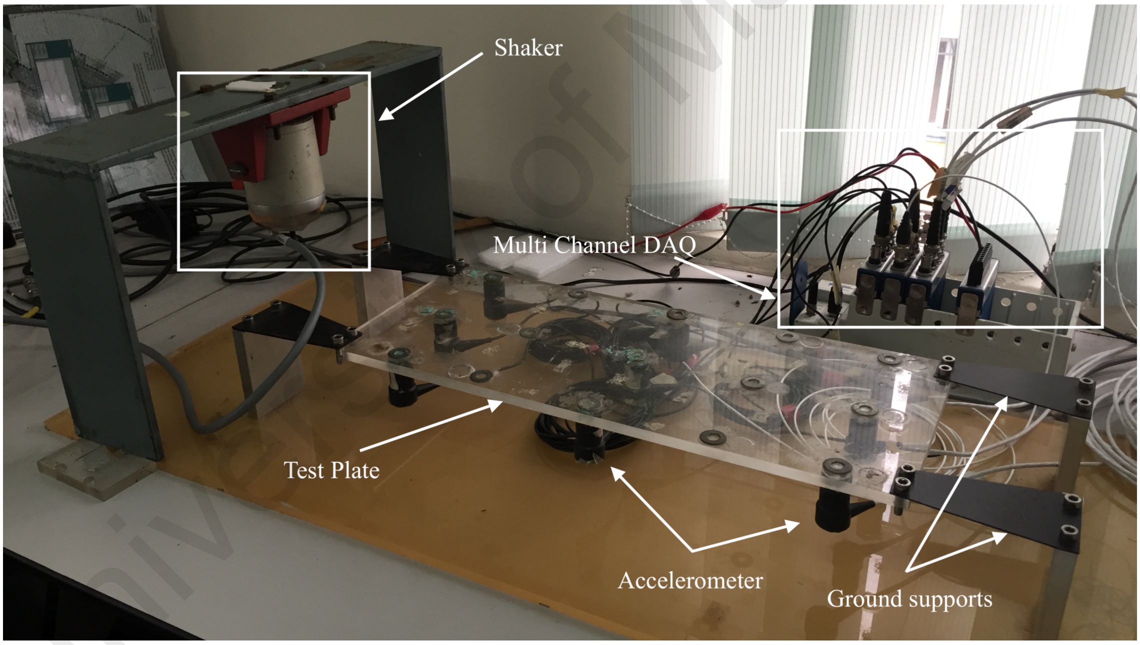

Figure 3.1: Experimental setups for damage identification study

The plate was ground supported using nut and bolt at each of the four corners. It was connected to the steel plate and aluminium supports at every corners as shown in Figure 3.2. The ground supports acted as the suspension/spring components of a typical car wheels. Nine (9) accelerometers were mounted in symmetric order on the plate to acquire the vibration responses done by the impact hammer. Previous studies used four (4) to nine (9) sensors (Worden & Staszewski, 2000; Haywood et al., 2004; LeClerc et al., 2007), as for this experiment a maximum number of sensors; nine (9) sensors for EMA were taken since the objective of this project later is to reduce number of sensors needed without affecting the ANN performance.

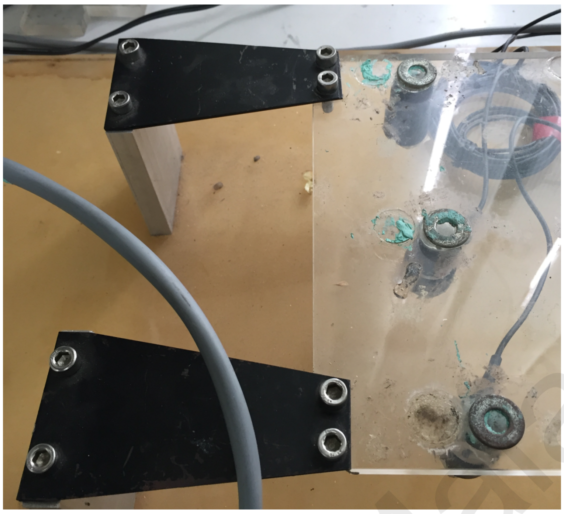

Figure 3.2: Ground supports of the plate

The accelerometer used in this experiment was a model S100C Wilcoxon Research: Integrated Circuit Pirzoelectric (ICP) accelerometer which has a built-in charge amplifier. This accelerometer is set to acquire vertical oscillation in this study and able to respond for 1-DOF vibration only. It has a sensitivity of 100mV/g along with a wide range of frequency of 0.5 to 10000Hz. The dimension of each accelerometer was 3.73 cm in height and 1.98cm in diameter. The mounting method used on the accelerometer is by cyanoacrylate adhesive which able to avoid any phase lag as shown in Figure 3.3 (SKF Condition Monitoring, 1999).

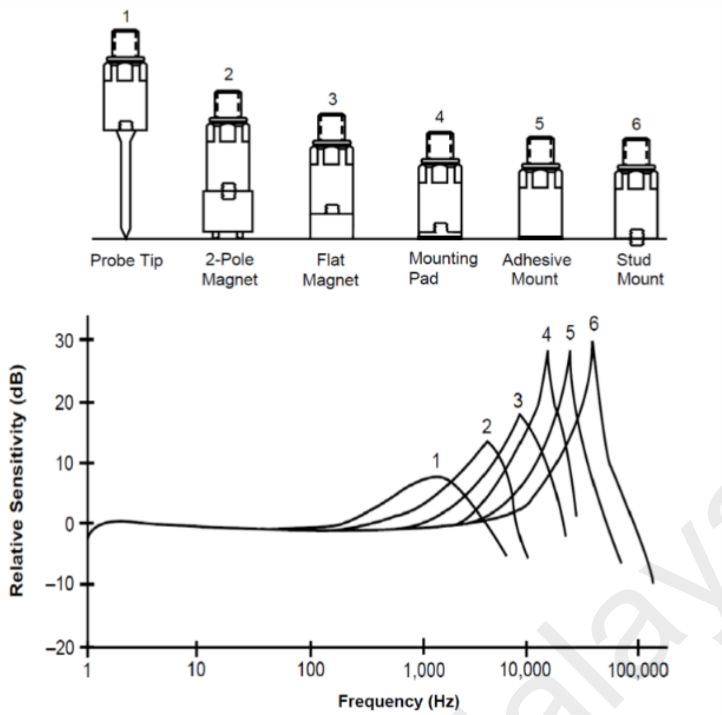

Figure 3.3: Accelerometer mounting methods vs effects on accelerometer's sensitivity (SKF Condition Monitoring, 1999)

A manual PCB impact hammer was used to create an impact on the plate structure for analysing its dynamic behaviour. It was used to measure the impacts which were done on vertical direction only. It has the sensitivity of 2.09mV/N and can measure up to ±2200N. As for the DAQ hardware system, National Instrument-Universal Serial Bus (NI-USB 9234) signal acquisition module was used in this setup to acquire ten (10) dynamic signals (1 impact hammer as input signal and 9 accelerometers as output signals). The DAQ hardware system will send the acquired data to the computer software, DASYLab v10.0 for the post-processing to acquire the FRF. The manual impact hammer was used in both EMA and ISMA experimental setup. As shown in Figure 3.4, the shaker's main objective was to create an operating/in-service system by producing the ambient forces to the structure and was only used in ISMA technique experiment. The shaker will not be used in EMA experiment. In this study, the shaker's motor frequency was set to 30Hz.

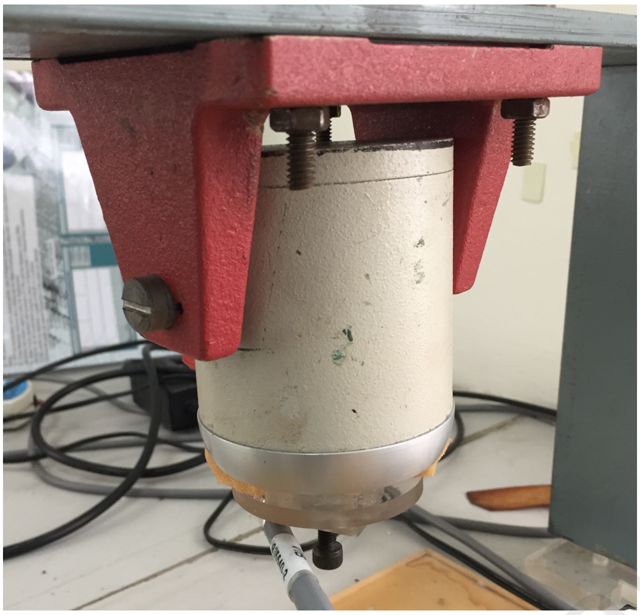

Figure 3.4: Shaker used to create an operating system environment

3.1.1 Data Acquisition Scheme

In order to generate the FRF, a data acquisition system was used called DASYLab. The impact done by the impact hammer will create a response from the accelerometer through the DAQ module which later recorded via DASYLab v10.0 software. The sampling rate and block size were the two main parameters in acquiring a signal during data acquisition. In order to select the appropriate sampling rate and block size, the frequency resolution or time resolution need to be considered. In this study, the sampling rate and block size were 2048 samples/sec (Hz) and 4096 samples respectively. This provides a frequency resolution of 0.5Hz and data acquisition time of 2 seconds. Both EMA and ISMA experiments used similar sampling rate and block size for the data acquisition.

3.2: Experiment Procedure

3.2.1 Experimental Modal Analysis (EMA)

In this experiment, the data processing to acquire the vibrational modal parameters (natural frequency and damping ratio) was not done because the modal parameters was not used to train the ANN model for damage identification scheme. Therefore, the experiment procedure were done up until acquiring the FRF data. Below are the brief procedure of EMA:-

1. Setting the desired measuring points

   The points which are selected to attach the accelerometer need to be well positioned enough to define the geometry of the structure, especially a complex structure.

2. Experimental apparatus set-up

   All the accelerometers along with the impact hammers are connected to the DAQ. The DAQ is connected to a PC to proceed with data processing.

3. Data acquisition through DAQ

   Done by using MDT-Q2 Data Acquisition System. The sensitivity of the accelerometer and the impact hammer need to be adjusted before proceed with any measurements. An average results are gathered and processed with DASYLab v10.0 to generate the FRF.

4. Data Processing

   To obtain the natural frequencies and mode shapes of the structure extracted from the FRF.

3.2.2 Impact-Synchronous Modal Analysis (ISMA)

The experimental setup and procedure for ISMA were different in terms of number of sensors used and signal processing and averaging technique. The number of sensors were reduced from nine (9) sensors to five (5) sensors. Also, ISMA was integrated with Impact-Synchronous Time Averaging (ISTA), utilized prior to performing the FFT operation to generate the FRF. When setting up the apparatus, the shaker was used and set to 30Hz in order to produce the ambient forces exist during operation. Besides, as mentioned above, the procedure was identical with EMA's procedure.

3.3: Damage Identification Methodology

3.3.1 Arrangements of sensors and damage location

Since the plate simulate a four-wheel car, the location of the damage usually happens at the suspension part where it absorbs the impact done by the tire when hitting a pothole or rough road. To simulate a damaged condition, the bolt and nut that hold the plate and ground supports together were used as the damage point. The nut will be unfasten or loosen to simulate the damage point, based on Figures 3.5 and 3.6, for example if the nut is loosen at point 1, it shows that damaged is done at point 1 (Front right tire suspension, assuming the left area plate is the frontal area of a car). Each point 1, 3, 7, and 9 consist of two (2) bolt and nuts, and both the nut will be loosen at the same amount degree of rotation. This will create four (4) damage locations. The bolt and nut for all four (4) damage locations were loosen up in equal amount degree of rotation, to an extent of shift in natural peaks were observed.

As shown in Figures 3.5 and 3.6, the number of sensors used in EMA and ISMA experiment varies to each other. In EMA used nine (9) sensors as for in ISMA only used five (5) sensors were reduced to only five (5) sensors. These creates two different approaches, EMA whereby the automobile during stationary and ISMA during operation. Assuming a scenario when the automobile during stationary, EMA technique is used to acquire the FRFs and trained on the ANN. The trained ANN with EMA FRFs dataset, it is then being used as ISMA FRFs testing dataset gathered when the automobile is moving or during operation. Since the plate is treat as an automobile, no sensor can be mounted on the wheel (Located at the edges of the plate; point 1, 3, 7 and 9) during operation. By mounting it on the body it is still possible to find the damages or loss of stiffness at the wheel or suspension. Though, for EMA the sensors were fixed to nine (9) sensors because sensor can be mounted on the wheel during stationary and one of the objective of this study is to study the reduction in number of sensors without affecting the performance accuracy. Later in this study will show the performance accuracy when the ANN is trained using nine (9) sensors (EMA dataset) and tested with (5) sensors (ISMA dataset). The impact done by the impact hammer can be done at certain point on the plate, also known as reference point. When the impact is done on point 2, 4, 5, 6, and 8, it will remove certain frequency vibration mode. This is because when the hammer hit at these points, it will not produce the low frequency mode which can relate to the vibration mode. Unlike point 1, 3, 7 and 9, when the impact hammer hits at these points it will produce the low frequency mode. As for this study, even though the FRF datasets were collected for reference point 1, 3, 7 and 9, the FRF dataset used to train the neural network for damage identification scheme was limited to FRF at reference point 1 only for both EMA and ISMA experiment. Each time an impact is done at point 1, it will produce nine (9) FRFs data from each of the nine sensors. Figures 3.5 and 3.6 show the arrangement of sensors and the damage locations for EMA and ISMA experiment, respectively.

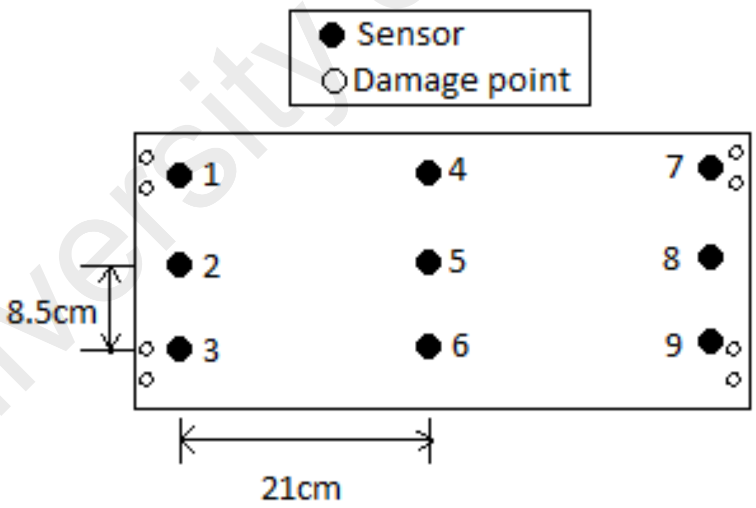

Figure 3.5: Sensor and damage location for EMA experiment

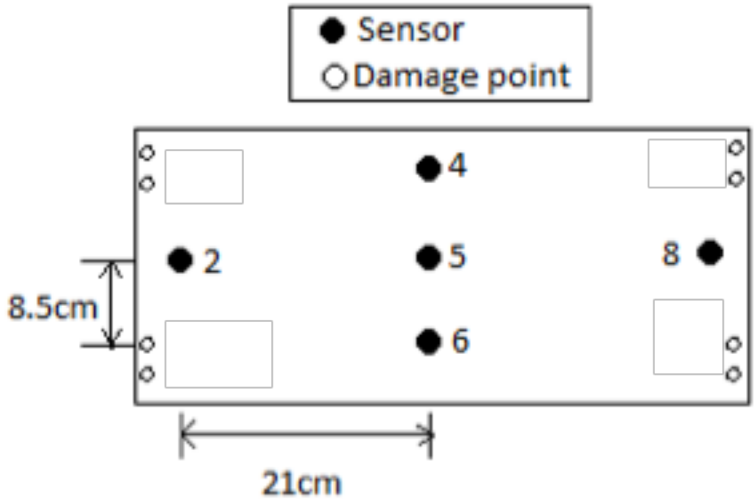

Figure 3.6: Sensor and damage location for ISMA experiment

During the data gathering phase, five output (5) conditions were created to classify the existence of the damage and its location. Table 3.1 shows the list of condition along with its description.

Table 3.1 List of conditions and description

Conditions	**Description**
Undamaged	All four (4) points of the nuts were tighten
Damaged1	Nuts at point 1 were loosen, as for point 3, 7, and 9 were tighten
Damaged2	Nuts at point 3 were loosen, as for point 1, 7, and 9 were tighten
Damaged3	Nuts at point 7 were loosen, as for point 1, 3, and 9 were tighten
Damaged4	Nuts at point 9 were loosen, as for point 1, 3, and 7 were tighten

3.3.2 Frequency domain feature (FRF) data arrangement

In this research project, the FRFs data were collected from two different experiment techniques, EMA and ISMA. For the EMA technique, five (5) averages were gathered during the experiment which later will be used to train the neural network. This is because the higher the number of samples used to train the neural network, the better the neural network will perform especially when the number of sensors are reduced to a single sensor.

As for the ISMA technique, the FRFs taken from the averaged ISTA to remove the ambient sound produce a single average. As for the ISMA technique, only one (1) average were used and the samples will be used to test the neural network. This later can provide another findings to prove that ISMA has the same effectiveness as the EMA technique. Table 3.2 shows the total number of FRFs collected from two different modal analysis technique. For EMA, five (5) number of averages will be collected from each of the nine (9) sensors for each condition, generating total number of 225 FRFs. As for ISMA, only five (5) sensors were being used to collect the FRF for each condition, generating total number of 25 FRFs.

Table 3.2: Total number of FRFs collected from two different modal analysis technique

Modal Analysis Technique	**EMA (During Stationary)**	**ISMA (During Operation)**
Sensors Location (Point)	1, 2, 3, 4, 5 ,6, 7, 8 ,9	2, 4, 5, 6, 8
Number of averages	5	1
Number of sensors	9	5
Number of conditions	5	5
Total number of FRFs (Average x Sensor x Condition)	225 FRFs	25 FRFs

Each FRF gathered from the accelerometer and DAQ were set to provide the magnitude (g/N) of frequency starting from 0 Hz up until 1023.5 Hz. Though, this study will only cover the frequency range from 0 Hz up until 199.5 Hz, which consist of 5 mode shapes. As stated earlier, the frequency resolution and data acquisition time 0.5 Hz and 2s respectively, in DASYLab v10.0. Since the frequency resolution was 0.5 Hz, every 1 Hz will produce two (2) FRF outputs magnitude. Thus, with the frequency range from 0 Hz to 199.5 Hz, the total number of output produced for each FRF will be 400 outputs. Table 3.3 shows the number of samples collected from two different modal analysis.

Table 3.3: Number of samples collected from two different modal analysis technique

Modal Analysis Technique	EMA (During Stationary)	ISMA (During Operation)
Total number of FRFs (Average x Sensor x Condition)	225 FRFs	25 FRFs
Frequency Range	0 Hz – 199.5Hz	
Total number of outputs/FRF	200 x 2 = 400	
Number of Samples (Total number of FRFs x Total number of outputs/FRF)	225 FRFs x 400 = 90,000 samples	25 FRFs x 400 = 10,000 samples

3.3.3 ANN implementation

Python language was used to model and train the neural networks in order to identify damage. Python language has been well-known for applying machine learning, having the most powerful open-source libraries in the world. The top numerical platform for neural network are Theano and TensorFlow. Both are the most powerful libraries and widely used in deep learning research and development, but it can be difficult to use directly for creating a neural network or deep learning models. This is where Keras library comes in, Keras Python library able to provide the most user-friendly way to create a range of neural network models by using Theano or TensorFlow as the backend library. It able to run on both Python 2.7 or 3.5 version and execute on CPUs and GPUs given the underlying frameworks. Keras API library was developed and maintained using these four (4) guiding principles (Brownlee, 2018):

- Minimalism (User-friendly): It provides sufficient enough to achieve an outcome with no frills and maximizing readability.
- Modularity: It can be understood as sequence alone and the model are discrete components that can be combined in arbitrary ways.
- Extensibility: New components can be added fast and easily within the framework, in order trial and explore new ideas.
- Python: All the model files is in native Python.

Deep learning is never been easier with Keras library, making it more widely used for those who just started learning about deep learning. Nowadays with abundant amount of data, deep learning is the most powerful data-driven machine learning tool that can be applied to any industry.

The vital data structure of Keras is a model; a way to organize layers. The simplest model in Keras is the *Sequential* model, a linear stack of layers:

from keras.models import Sequential

model = Sequential()

In order to stack a layer, it uses *.add* to the model, *Dense* type layer as follows:

from keras.layers import Dense

*model.add(Dense(units=**a**, activation='relu', input_dim=**b**))*

*model.add(Dense(units=**c**, activation='softmax'))*

The second line shows the shape of the input, giving ***b*** number of inputs (neurons) and ***a*** number of neurons of hidden layer. As for the third line shows the output layer with ***c*** number of neurons. Keras supports a wide range of neuron activation function such as softmax, rectifier, logistic, hyperbolic tangent (*tanh)* and sigmoid. For the hidden layers in this study, the model uses rectifier (*relu*), shown in equation 3.1, activation since it speeds up the training process with a very simple gradient computation and computational step.

$$\text{Rectifier: } f(x)=max(0,x) \qquad (3.1)$$

As for the last layer, softmax, shown in equation 3.3, is used when ‘n’ number of classes for classification problem. Binary classification whereby n=2, can use both sigmoid and softmax activation on the last layer for classification problem. As for multi-class classification problem, softmax is the kind where the function, the sum of all softmax units are supposed to be 1, unlike in sigmoid. In multi-class classification, the outputs are dependent of one another and increasing the output value of one class makes the others go down (sigma=1) making the softmax more preferred choice. Sigmoid equation is shown in equation 3.2.

$$\text{Sigmoid: } S(t) = \frac{1}{1+e^{-t}} \qquad (3.2)$$

$$\textit{Softmax: } h_0(x) = \frac{1}{1+exp\,(-\theta^T x)} \qquad (3.3)$$

3.3.4 ANN Model Validation

There are a lot of ways and decisions to make in designing the ANN model architecture. Though, it is important to have a robust way of evaluating the performance of ANN model. There are several methods to evaluate a model performance using Python. Before stating the method, it is important to define the meaning of training dataset, validation dataset and also test dataset. Below are the definition for each dataset:-

- Training Dataset: The sample of data used to fit the model.
- Validation Dataset: The sample of data used to provide an unbiased evaluation of a model fit on the training dataset while tuning model hyperparameters. The evaluation becomes more biased as skill on the validation dataset is incorporated into the model configuration.
- Test Dataset: The sample of data used to provide an unbiased evaluation of a final model fit on the training dataset.

Below are the techniques used to evaluate a model performance:-

1) Train/Test method

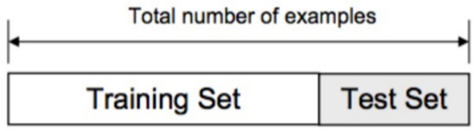

Figure 3.7: Train/Test method

Train/test method is the simplest technique that can be used to evaluate a model as shown in Figure 3.7. This technique is not as robust as cross validation because of randomness happened when splitting the dataset into a training dataset and a validation or test dataset. Each time when splitting the total number of samples dataset, the datasets will not be split the same as the previous ones. For example, what if one sub of the data has only FRF from certain conditions; the training dataset consist of only undamaged, damaged1 damaged2, damaged4 and testing dataset consist of damaged3 only. Keep in mind each time the program is rerun/retrain the ANN, it will split the train and test dataset differently as the previous ones. Thus, this will produce inconsistency results of the model performance. The other way around in applying this technique is by multiple split tests and take the average model performance from the overall. The inconsistency results of the model performance only happened if the data splitting is done by the Python program itself, whereby the user needs to input the train and test datasets split percentage size. If the train and test datasets are from two different sources, not split by the Python program, it can produce consistent results of the model performance (Used in ISMA FRF validation).

In this study, train/test method was only being used in showing the damage identification scheme and ISMA FRF validation. Figure 3.8 shows the train/test split method in damage identification scheme. The EMA dataset will be split by the Python program to 0.7/0.3, 70% for the training dataset, and 30% for the testing dataset. The reason why train/test method was used in damage identification scheme was because it is the only way to show the output results for the damage identification scheme.

As for the ISMA FRF validation shown in Figure 3.9 below, the ANN will be trained using EMA FRF datasets, and tested with ISMA FRF datasets. In this case, this project can validate the ISMA FRF dataset whether it has similar FRF as the EMA with similar experimental setup.

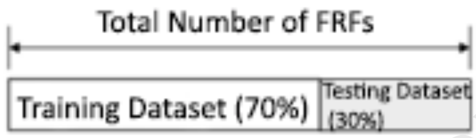

Figure 3.8: Train/Test method in Damage Identification Scheme using EMA dataset

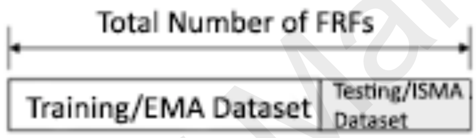

Figure 3.9: Train/Test method in ISMA FRF validation

2) Cross-validation (CV)

A solution to the problem of ensuring each instance is used for training and testing and equal number of times while reducing the variance of performance score is to use cross validation. K-fold cross-validation is common CV technique, where k is the number of splits to make in the dataset. Figure 3.10 shows an example of how k-fold cross-validation split the training dataset and test dataset. In this case, it will split the dataset into 4 parts (4 folds) and the NN model will be running for 4 times. Each time the model run, it will be trained on 75% of the dataset and tested on another 25% , and the next run of the test dataset will not be the same as the previous ones. This validation is more robust than the normal train/test method.

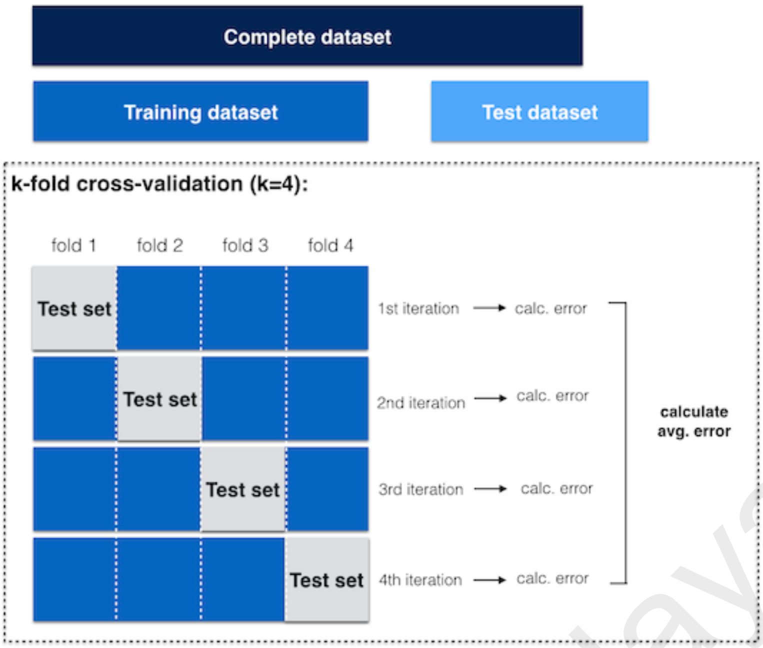

Figure 3.10: 4-fold cross-validation technique

In this study, 10-fold cross-validation (k=10) was used to evaluate the performance of the ANN model. The complete dataset used was the EMA FRF dataset, which will be split as much as 10-fold, calculate its percentage error for each fold and generate the averaged error. The CV method will be used throughout this study to evaluate the performance of ANN model in parameters tuning and reducing number of samples by reducing the number of sensors and frequency range, to ensure the damage identification scheme is robust enough to predict future FRFs dataset.

3.3.5 ANN Architecture

As stated earlier, the Keras simplest model which being widely used is the *Sequential* model. This study used the Multi-layer Perceptron (MLP), a feedforward network consists of at least three (3) layers of nodes. As for the learning algorithm, MLP utilized the supervised technique called backpropagation technique. Figure 3.11 shows the artificial neural network architecture that was being used in this study.

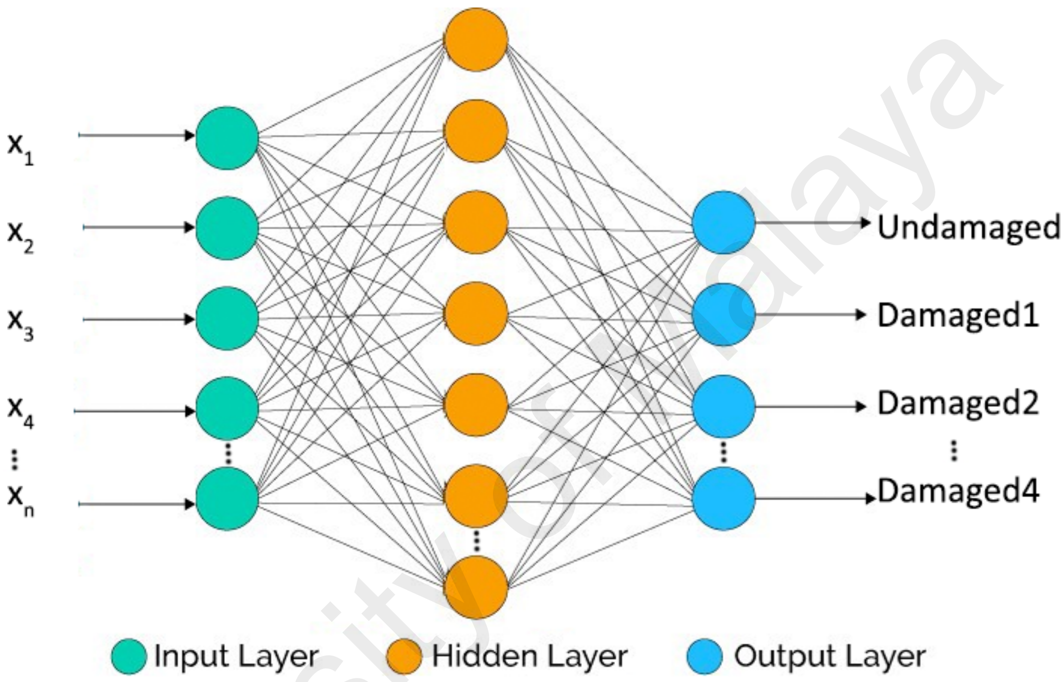

Figure 3.11: Neural network architecture

The number of neurons, n, of the input layer depends on the number of outputs that were produced by each FRF. As stated in Table 3.3 earlier, the number of outputs produced were 400 outputs. Therefore, the number of neurons of the input layer was n=400 neurons, x_{400}. Though, the number of input layer will vary when the frequency range is reduced later in this study for optimization purpose. The training and testing FRF datasets need to have equal number of total outputs/FRF since both datasets will use the ANN model. Similarly with the output layer which consists of five (5) neurons, which depends on the number of output conditions that were being created. It can be observed in Figure 3.11 that the outputs are the conditions for the damage identification scheme that were set earlier. Therefore, the ANN model required one full FRF to produce the output result.

The ANN model parameters tuning was done by adjusting the number of neurons and hidden layers to find the optimized ANN model. The model performance was evaluated using 10-fold cross-validation method and EMA FRF dataset was used. Table 3.4 shows the ANN model parameters tuning on the number of neurons of the 1st hidden layer. It shows that as the number of neuron increases, the performance of the ANN model increases. Though, the performance reached the maximum percentage of 100% with twenty (20) neurons at the 1st hidden layer. The performance of the NN will be similar as twenty (20) neurons even after the number of neurons were added more than twenty (20). It is proven from 20 up until 25 neurons, it produced the same performance accuracy. Since with a single hidden layer the model managed to produce a 100% performance accuracy, there will be no reason to add a second (2nd) hidden layer. Therefore, the optimized ANN model will have twenty (20) neurons at the 1st hidden layer (single hidden layer). The optimized ANN model will be used to record the output results (damage identification) showing how well the model predict and identify the damage and its location.

Table 3.4: ANN model parameters tuning on the number of neurons of the hidden layer

1st Hidden Layer	10-fold Cross-validation	
Number of neurons	Percentage Error (%)	Performance Accuracy (100% - % Error = %)
1	74.31%	25.69%
2	60.04%	39.96%
3	56.15%	43.85%
4	34.86%	65.14%
5	34.25%	65.75%
6	24.15%	75.85%
7	14.58%	85.42%
8	6.36%	93.64%
9	5.83%	94.17%
10	4.49%	95.51%
11	7.65%	92.35%
12	1.80%	98.20%
13	1.34%	98.66%
14	1.80%	98.20%
15	0.43%	99.57%
16	0.91%	99.09%
17	0.91%	99.09%
18	0.89%	99.11%
19	0.89%	99.11%
20	0.00%	100.00%
21	0.00%	100.00%
22	0.00%	100.00%
23	0.00%	100.00%
24	0.00%	100.00%
25	0.00%	100.00%

Figures 3.12 and 3.13 show the output given on the python software, based on different number of neurons at the 1st hidden layer. The first line shows the backend that, Tensorflow, was being used for the neural network. The user need to input the number of neurons for the 1st hidden layer. It will then print the dataset shape of the comma separated value (csv) EMA dataset file. Dataset shape is defined as (number of rows, number of columns). In the Figures 3.12 and 3.13, it stated that that dataset shape is (225, 401), consist of 225 row of FRFs and 401 columns (400: number of outputs/FRF, 1: the last column is the condition output for each of the FRF). Lastly, the baseline is the performance accuracy percentage for the model along with the program running time. It can be observed that the program running time increases as the number of neurons at the 1st hidden layer increases.

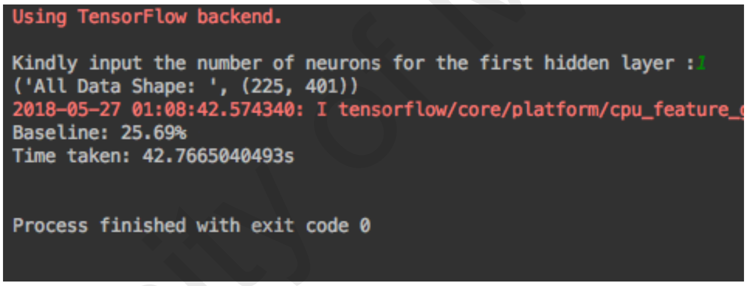

Figure 3.12: With a single neuron at the 1st hidden layer output

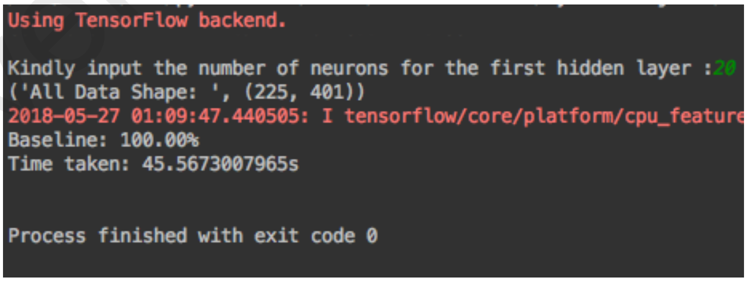

Figure 3.13: With 20 neurons at the 1st hidden layer output

As stated earlier, there are different types of activation functions that can be used on the neural network. The activation function that was used for the first two layers are the rectifier (*relu*) activation function since it produced better performance than Logistic and Hyperbolic tangent (*tanh)*. As for the output layer, softmax activation function was used for multi-class classification problem (5 conditions). Next step will be compiling the NN model which uses the numerical libraries such as Theano or TensorFlow, and TensorFlow backend was chosen. Loss function is needed in order to evaluate a set of weights, the optimizer used to search through different weights for the network and any optional metrics to collect and report during training. Logarithmic loss was used in compiling as defined in Keras as "*categorical_crossentropy*" for multi-class classification problem. There are also *binary_crossentropy* which is used for binary classification problem. A efficient gradient descent algorithm called "*adam*" was used since it is an efficient default in Keras. The number of iterations were set at two hundred (200) iterations and the batch size was twenty five (25).

Chapter 4: Results and Discussions

4.1: FRF Analysis

Figure 4.1 shows the EMA FRFs sample for Undamaged condition during stationary dataset. Each peak shows the natural frequency of the plate structure whereby when the structure vibrates at that frequency, it will result in resonance.

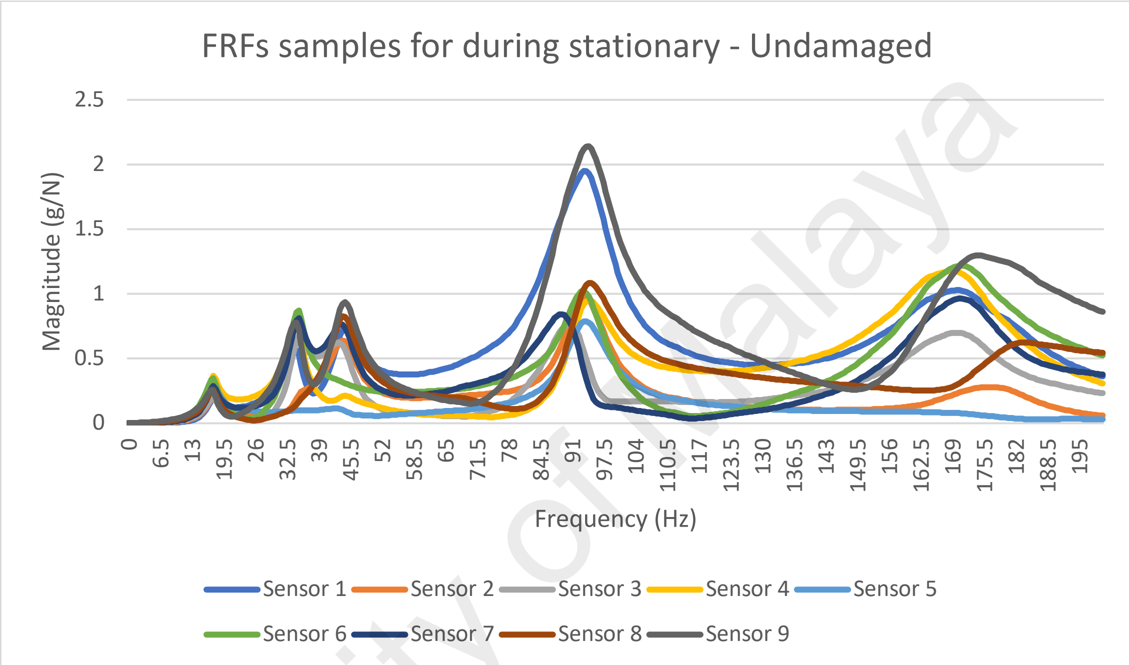

Figure 4.1: FRFs samples for during stationary - Undamaged

As stated earlier there were five (5) conditions designed for this damage identification scheme. Each condition produced different FRFs data and graph pattern. With the help of ANN, it is convenient to study the FRFs graph pattern for each condition and classify it into each of its condition. Figure 4.2 shows the FRFs graph for each of the conditions for EMA FRFs and Figure 4.3 for ISMA FRFs.

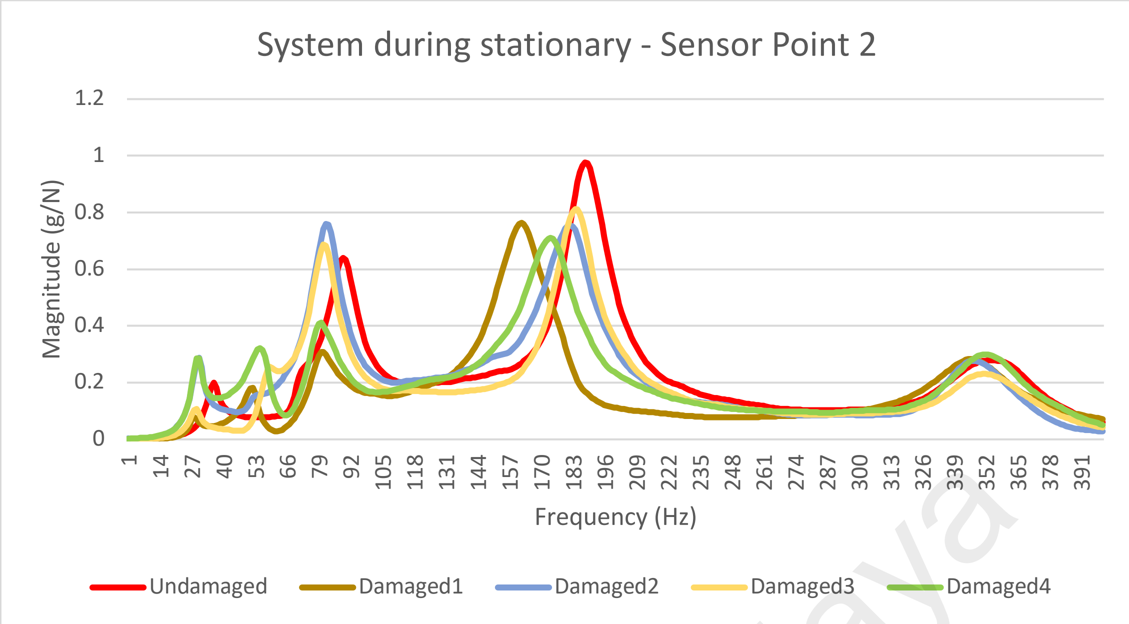

Figure 4.2: FRFs graph for system during stationary (EMA) – Sensor Point 2

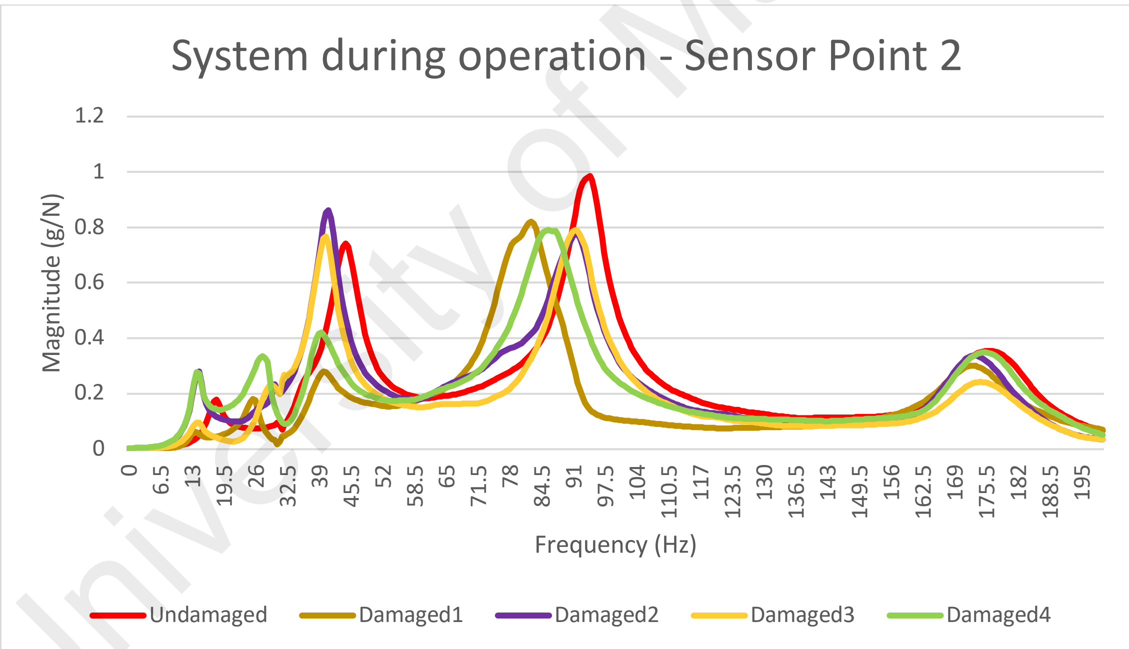

Figure 4.3: FRFs graph for system during operation (ISMA) – Sensor Point 2

Based on both Figures 4.2 and 4.3, it can be observed that when the structure is damaged, the FRFs graph are shifted to the left side towards lower frequency range. The most right side will be the undamaged FRF, showing when a structure is damaged the dynamic characteristics will changed. Moreover, both EMA and ISMA datasets produced almost identical FRFs pattern.

Figures 4.4, 4.5, 4.6, 4.7, and 4.8 show the system during operation (ISMA) FRFs for each condition on all sensor points. It can be seen that the magnitude for each vibration mode varies for different conditions. For example in Figure 4.5, FRFs for Damaged1 condition has the highest magnitudes for the 2nd, 4th and 5th vibrations modes and having the least magnitude for the 1st and 3rd vibration modes. This can relate to the vibration response of each mode shape when there is a change in structure properties. In Figure 4.8, FRFs for Damaged4 condition has the optimal magnitude for all of their vibration mode, making it the most balanced and easy to identify if damage happened at that point.

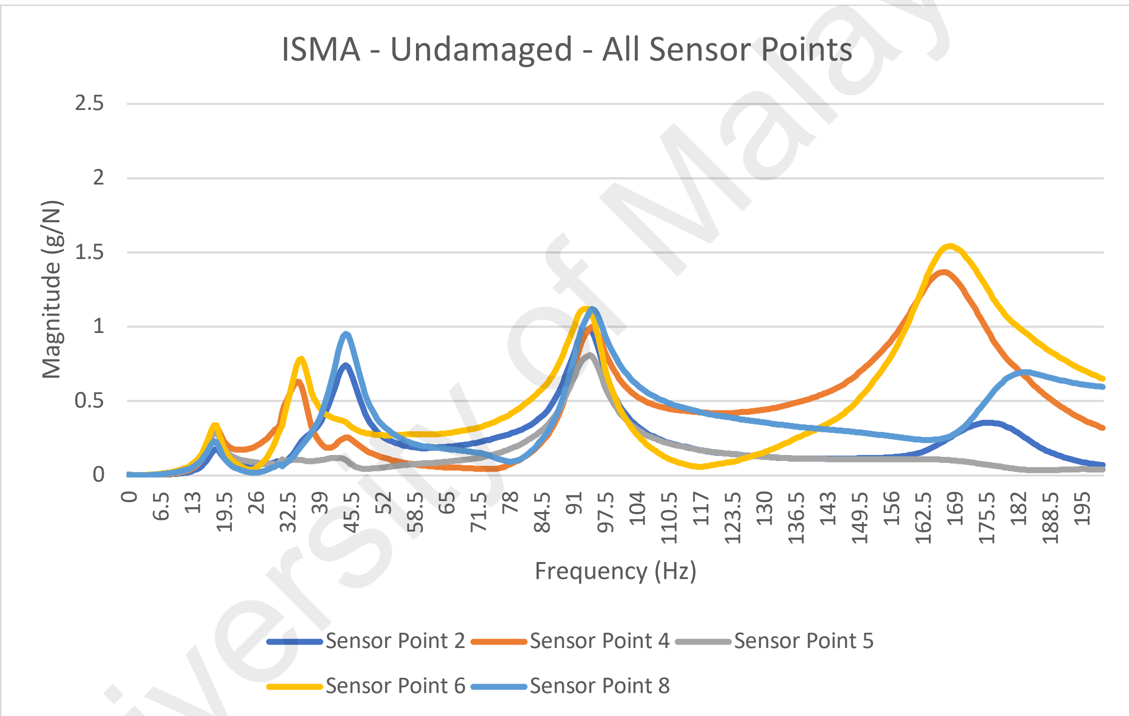

Figure 4.4: ISMA FRFs for Undamaged condition on all sensor points

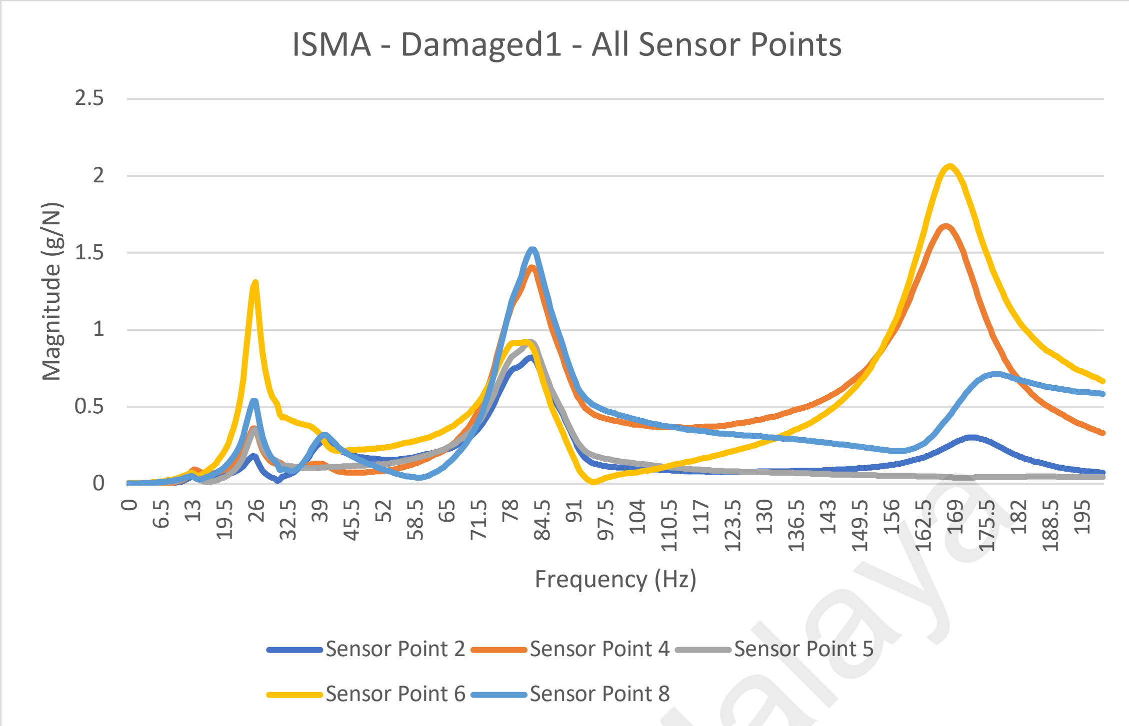

Figure 4.5: ISMA FRFs for Damaged1 condition on all sensor points

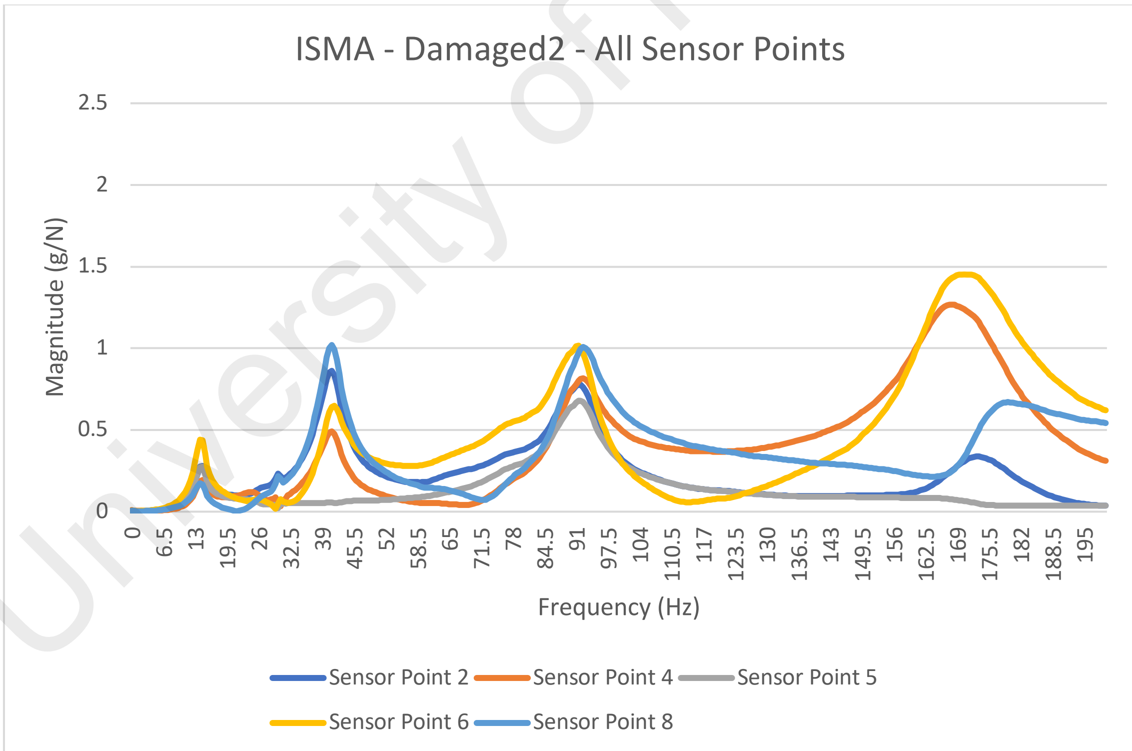

Figure 4.6: ISMA FRFs for Damaged2 condition on all sensor points

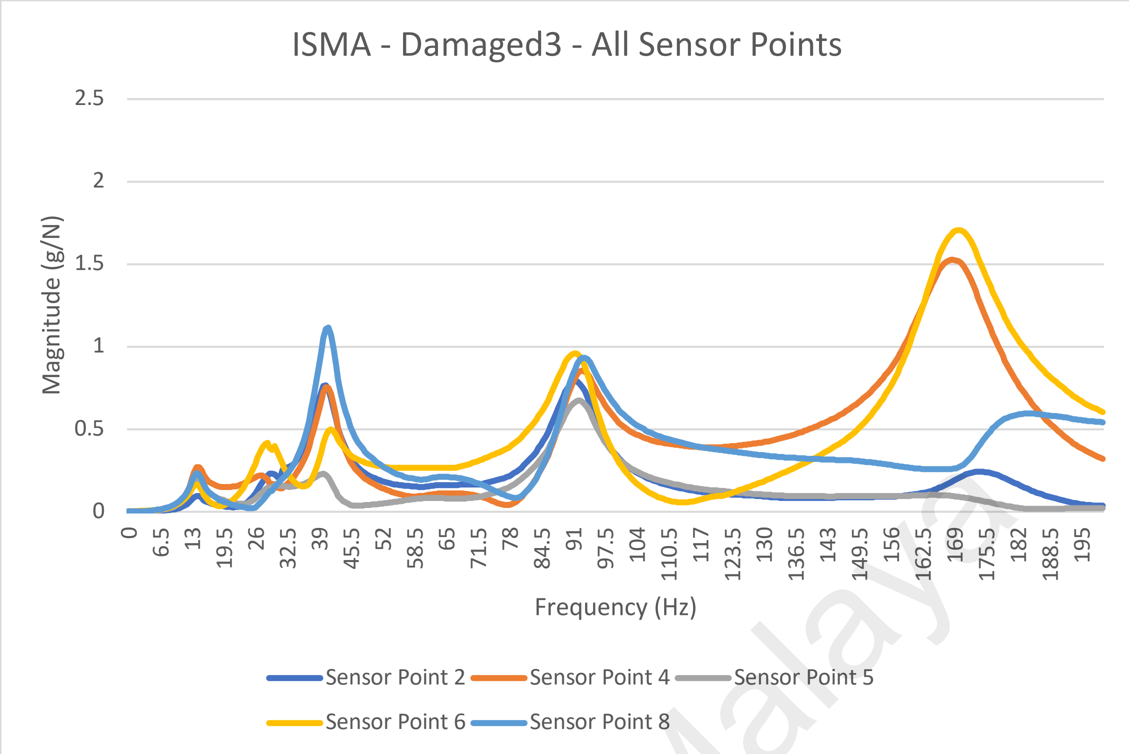

Figure 4.7: ISMA FRFs for Damaged3 condition on all sensor points

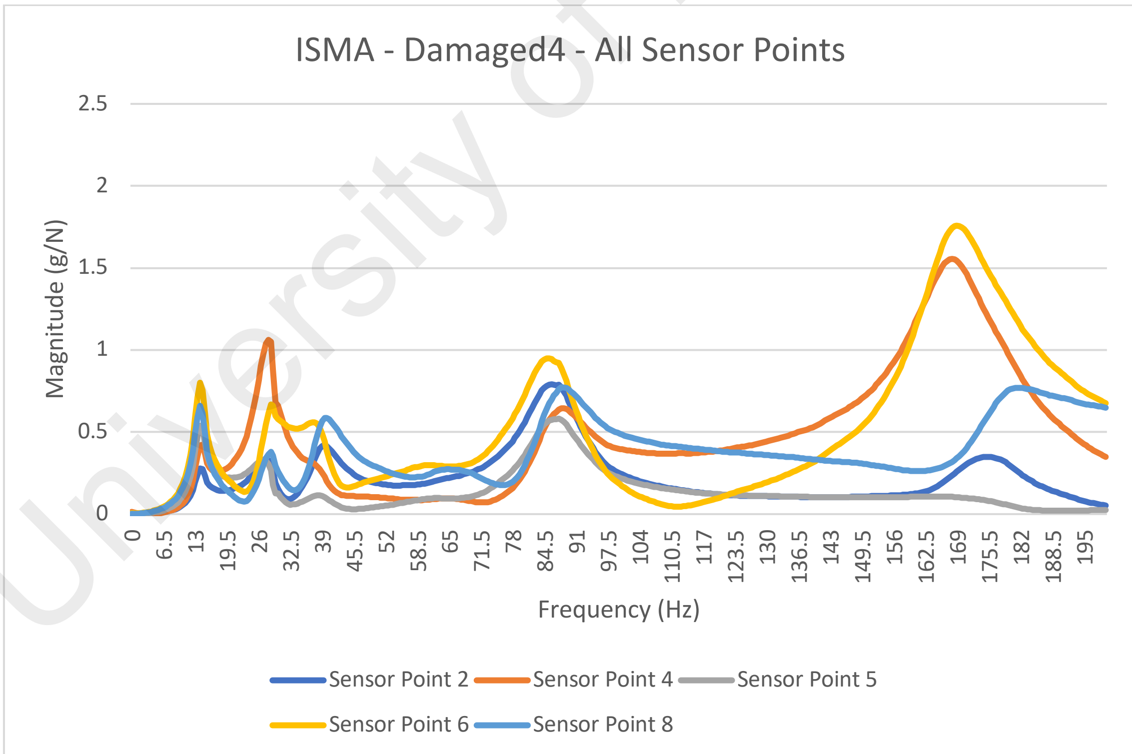

Figure 4.8: ISMA FRFs for Damaged4 condition on all sensor points

4.2: Damage Identification Scheme

In this section will show the output results for damage identification scheme using ANN. Since the approach that was used in this damage identification problem is classification problem, it is suitable to present the output results in form of F1 score. F1 score is a measure of a test's accuracy by considering both the precision *p* and recall *r* of the test to compute the score, *F1* as shown in equation 4.1. *P* is the number of correct positive results divided by the number of all positive results returned by the classifier, and *r* is the number of correct positive results divided by the number of all relevant samples (all samples that should have been identified as positive). The F1 score is the harmonic average of the precision and recall, where an F1 score reaches its best value at 1 (perfect precision and recall) and worst at 0 (Wikipedia, n.d.)

$$F_1 = \frac{2}{\frac{1}{\mathrm{recall}} + \frac{1}{\mathrm{precision}}} = 2 \cdot \frac{\mathrm{precision} \cdot \mathrm{recall}}{\mathrm{precision} + \mathrm{recall}} \quad (4.1)$$

Also, the approach used to evaluate the performance was by splitting the EMA dataset using the Python program and test/train method. Table 4.1 shows the number of samples used to train and test the ANN model by splitting the EMA dataset to 70/30.

Table 4.1: EMA dataset arrangement and number of samples used

EMA Dataset	Number of FRFs	Percentage (%)	Number of samples (FRF x 400 outputs/FRF)
Overall FRFs	225	100%	90000
Training FRF Dataset	157	70%	62800
Testing FRF Dataset	68	30%	27200

Figure 4.9 shows the output results from the Python program. It shows the dataset shape for the overall, training and testing along with the classification report. It can be seen that the dataset shape for both training and testing consist of five (5) columns. This is because

the condition output for each FRF (the last column in overall dataset) was convert from a categorical (undamaged, damaged1, damaged2, damaged3 & damaged4) to numerical. It was done by using the One-Hot Encoding method whereby the outputs are represent in form of binary variable “0” means FALSE and “1” means TRUE, as shown in Figure 4.9 and Table 4.2. The classification report shows the precision, recall, f1-score and the support. In this case, the support is the number of FRFs for each condition that were tested on the ANN model. The total number of supports are 68, equal with the number of FRFs showed in Table 4.1. It can be observed that the F1-score for all the conditions are 1.00, resulting with an average F1 score of 1.00. Figure 4.10 shows the F1 score in form of visual for each of the tested conditions. The example of calculation for both precision and recall are shown below (Undamaged, Damaged1 & Damaged4): -

$$precision = \frac{13}{13} = 1.00$$

$$recall = \frac{13}{13} = 1.00$$

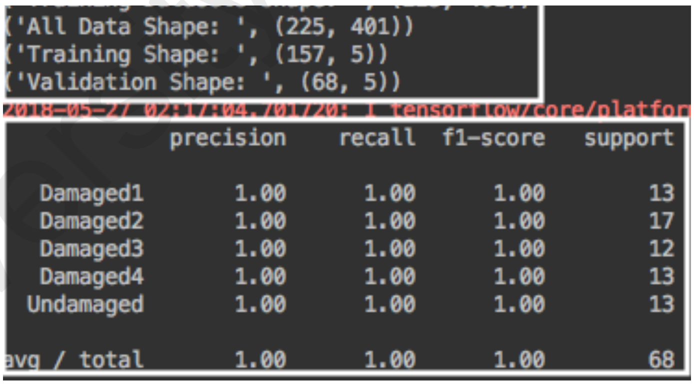

```
('All Data Shape: ', (225, 401))
('Training Shape: ', (157, 5))
('Validation Shape: ', (68, 5))
2018-05-27 02:17:04.701720: I tensorflow/core/platfor
             precision    recall  f1-score   support

   Damaged1       1.00      1.00      1.00        13
   Damaged2       1.00      1.00      1.00        17
   Damaged3       1.00      1.00      1.00        12
   Damaged4       1.00      1.00      1.00        13
  Undamaged       1.00      1.00      1.00        13

avg / total       1.00      1.00      1.00        68
```

Figure 4.9: Output results from the Python program

Once both precision and recall are calculated, the values will be substituted to equation 4.1 to acquire the F1 score for each condition.

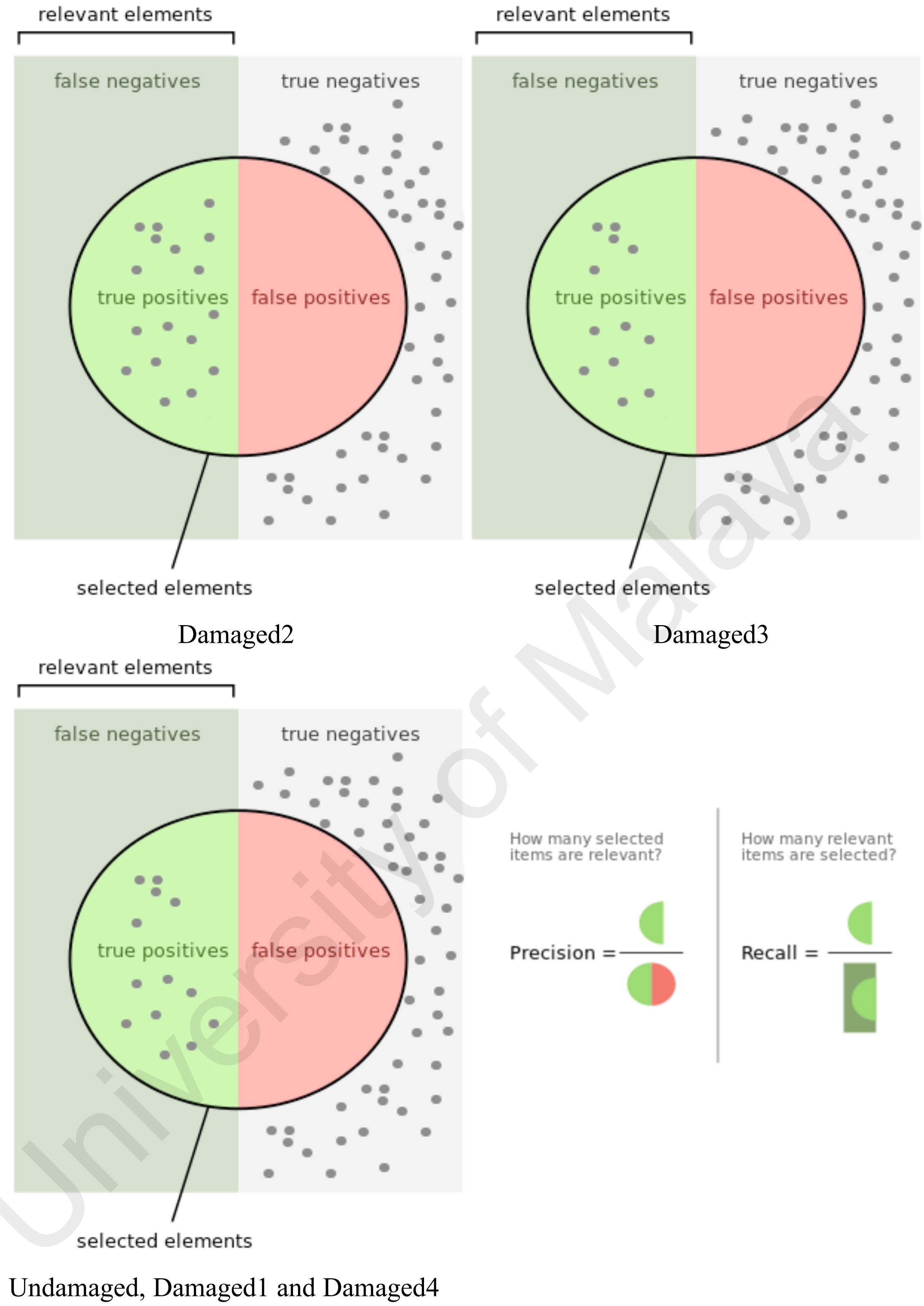

Figure 4.10: F1-score classification results

For more in-depth clarification, Figure 4.11 shows the predicted output and actual output for all testing dataset acquired from the Python program. It can be seen the outputs are in form of one-hot encoded, whereby the “0” column is damaged1, “1” column is damaged2, “2” column is damaged3, “3” column is damaged4 and lastly “4” column is undamaged. From here the data is extracted into Microsoft Excel and produce a table consist of all the 68 testing FRFs output results as shown in Table 4.2. It can be observed that the “True” outputs are highlighted in green as for the “False” outputs are highlighted in red.

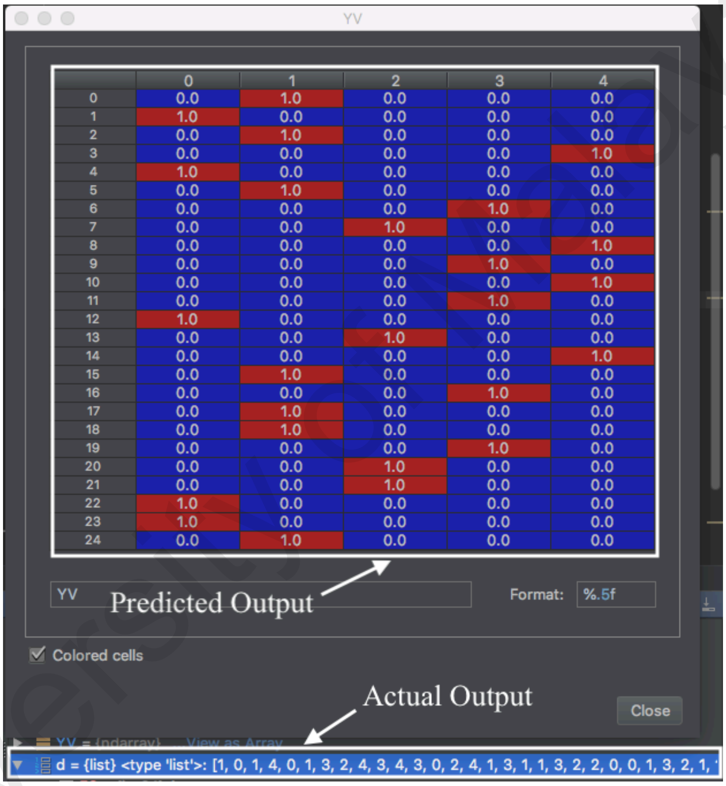

Figure 4.11: One-hot encoding results for predicted output and actual output

With these findings, it proved that a robust damage identification scheme by using the EMA FRF datasets with ANN is designed. The next section will test the ISMA FRF dataset on a trained ANN model by EMA dataset for validation.

Table 4.2: Testing FRFs output results in form of one-hot encoded

No of Testing FRFs	Actual Output					Predicted Output				
	Damaged1	Damaged2	Damaged3	Damaged4	Undamaged	Damaged1	Damaged2	Damaged3	Damaged4	Undamaged
1	0	1	0	0	0	0	1	0	0	0
2	1	0	0	0	0	1	0	0	0	0
3	0	1	0	0	0	0	1	0	0	0
4	0	0	0	0	1	0	0	0	0	1
5	1	0	0	0	0	1	0	0	0	0
6	0	1	0	0	0	0	1	0	0	0
7	0	0	0	1	0	0	0	0	1	0
8	0	0	1	0	0	0	0	1	0	0
9	0	0	0	0	1	0	0	0	0	1
10	0	0	0	1	0	0	0	0	1	0
11	0	0	0	0	1	0	0	0	0	1
12	0	0	0	1	0	0	0	0	1	0
13	1	0	0	0	0	1	0	0	0	0
14	0	0	1	0	0	0	0	1	0	0
15	0	0	0	0	1	0	0	0	0	1
16	0	1	0	0	0	0	1	0	0	0
17	0	0	0	1	0	0	0	0	1	0
18	0	1	0	0	0	0	1	0	0	0
19	0	1	0	0	0	0	1	0	0	0
20	0	0	0	1	0	0	0	0	1	0
21	0	0	1	0	0	0	0	1	0	0
22	0	0	1	0	0	0	0	1	0	0
23	1	0	0	0	0	1	0	0	0	0
24	1	0	0	0	0	1	0	0	0	0
25	0	1	0	0	0	0	1	0	0	0
26	0	0	0	1	0	0	0	0	1	0
27	0	0	1	0	0	0	0	1	0	0
28	0	1	0	0	0	0	1	0	0	0
29	0	1	0	0	0	0	1	0	0	0
30	0	0	0	1	0	0	0	0	1	0
31	1	0	0	0	0	1	0	0	0	0
32	0	0	1	0	0	0	0	1	0	0
33	0	0	1	0	0	0	0	1	0	0
34	0	0	0	1	0	0	0	0	1	0
35	1	0	0	0	0	1	0	0	0	0
36	0	0	0	1	0	0	0	0	1	0
37	0	0	1	0	0	0	0	1	0	0
38	0	0	1	0	0	0	0	1	0	0
39	1	0	0	0	0	1	0	0	0	0
40	1	0	0	0	0	1	0	0	0	0
41	0	1	0	0	0	0	1	0	0	0
42	0	0	0	0	1	0	0	0	0	1
43	0	0	0	0	1	0	0	0	0	1
44	0	1	0	0	0	0	1	0	0	0
45	1	0	0	0	0	1	0	0	0	0
46	0	1	0	0	0	0	1	0	0	0
47	1	0	0	0	0	1	0	0	0	0
48	0	0	0	1	0	0	0	0	1	0
49	0	1	0	0	0	0	1	0	0	0
50	0	1	0	0	0	0	1	0	0	0
51	0	0	0	0	1	0	0	0	0	1
52	0	0	0	0	1	0	0	0	0	1
53	0	0	0	1	0	0	0	0	1	0
54	0	0	0	0	1	0	0	0	0	1
55	1	0	0	0	0	1	0	0	0	0
56	0	0	1	0	0	0	0	1	0	0
57	0	0	0	0	1	0	0	0	0	1
58	0	0	1	0	0	0	0	1	0	0
59	0	1	0	0	0	0	1	0	0	0
60	0	0	0	0	1	0	0	0	0	1
61	0	0	0	0	1	0	0	0	0	1
62	0	1	0	0	0	0	1	0	0	0
63	0	1	0	0	0	0	1	0	0	0
64	0	0	1	0	0	0	0	1	0	0
65	0	0	0	0	1	0	0	0	0	1
66	1	0	0	0	0	1	0	0	0	0
67	0	0	0	1	0	0	0	0	1	0
68	0	0	0	1	0	0	0	0	1	0

4.2.1: ISMA FRF Validation

This section is to validate the ISMA FRFs to ensure it produce similar FRF pattern as the EMA when the system under testing is in operation. If the ISMA FRF testing dataset managed to produce a high performance accuracy on a trained ANN model by EMA FRF, it proved that the FRF that need to be used for the damage identification scheme are interchangeable between EMA and ISMA. Also, it is important to check the FRFs produced from ISMA experiment are valid by using the EMA FRF as benchmark dataset. Table 4.3 shows the number of samples used to train and test the ANN model by using EMA and ISMA dataset, respectively.

Table 4.3: FRF Dataset arrangement and number of samples used

Datasets	Number of FRFs	Number of samples (FRF x 400)
Training EMA FRF Dataset	225	90000
Testing ISMA FRF Dataset	25	10000

Figure 4.12 shows the output results from the Python program. It shows the dataset shape for the overall, training and testing along with the classification report. It can be observed that the F1-score for Undamaged, Damaged1 and Damaged4 are 1.00, Damaged2 is 0.91 and Damaged3 is 0.89, resulting with an average F1 score of 0.96. Figure 4.13 shows the F1 score in form of visual for each of the tested conditions. Figure 4.14 and Table 4.4 show the result outputs in Python program and extracted into table form, respectively. The calculation for precision for Damaged2 and recall for Damaged3 are shown below: -

$$precision(Damaged2) = \frac{5}{6} = 0.83$$

$$recall(Damaged3) = \frac{4}{5} = 0.80$$

It can be observed that the model wrongly classify the Damaged3's FRF as Damaged2. The possible reason behind the reduction of F1 score in this testing is because of different number of sensors being trained and tested on the ANN model. As stated earlier in the methodology, EMA and ISMA used 9 and 5 sensors respectively. Since the ANN model was trained using EMA datasets, this can lead to overfitting of the model based on 9 sensors dataset which consist of additional sensor locations. The additional sensor locations FRFs will affect the trained NN model in terms of performance when the testing dataset does not contain the additional sensor locations FRFs.

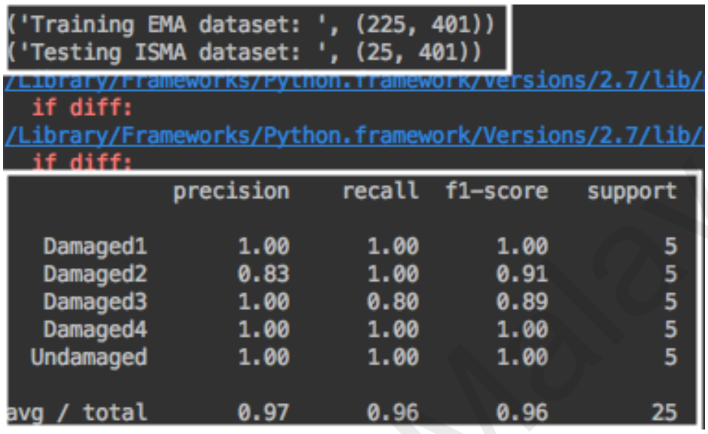

Figure 4.12: Output results from the Python program

Based on these findings, the main objective of this study is achieved by designing a damage identification scheme using both EMA and ISMA FRF data with ANN. Also, the ISMA FRF collected from the experiment during operation can be consider valid and usable for the damage identification scheme. The FRF dataset that need to be used for the damage identification scheme are also interchangeable for testing and training between EMA and ISMA.

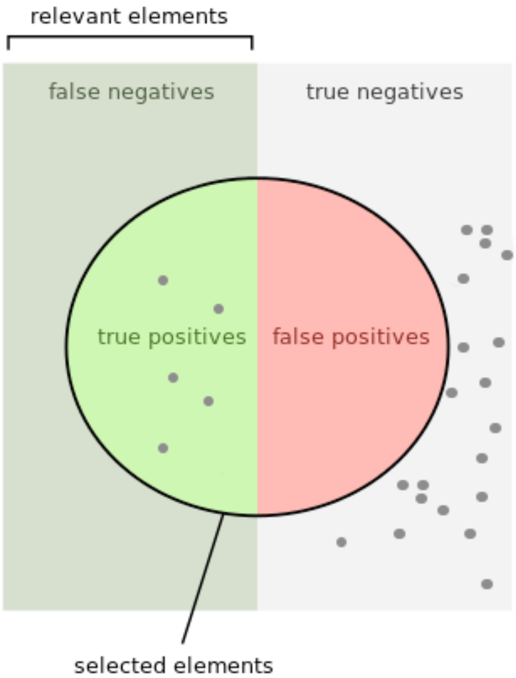

Undamaged, Damaged1 & Damaged4

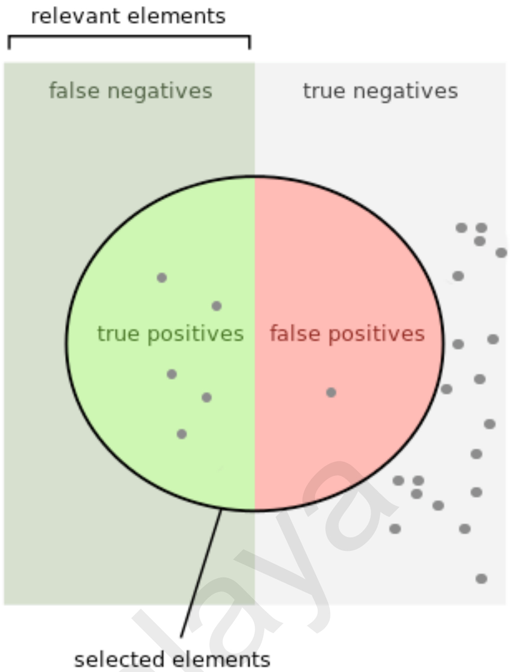

Damaged2

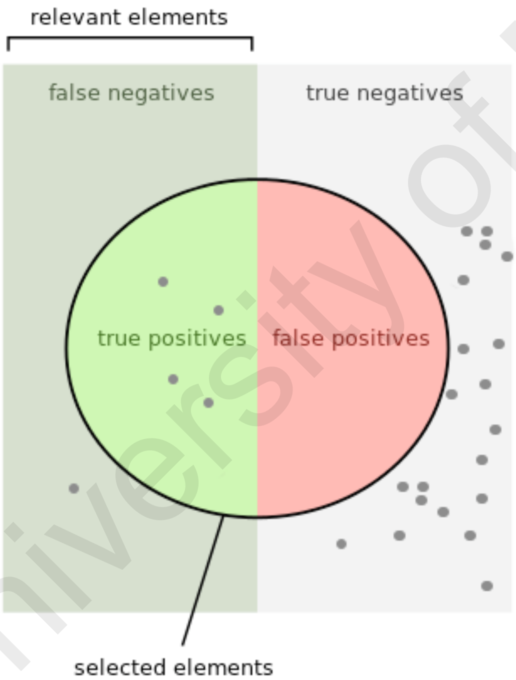

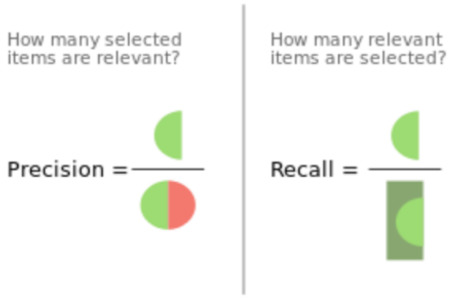

Damaged3

Figure 4.13: F1-score classification results

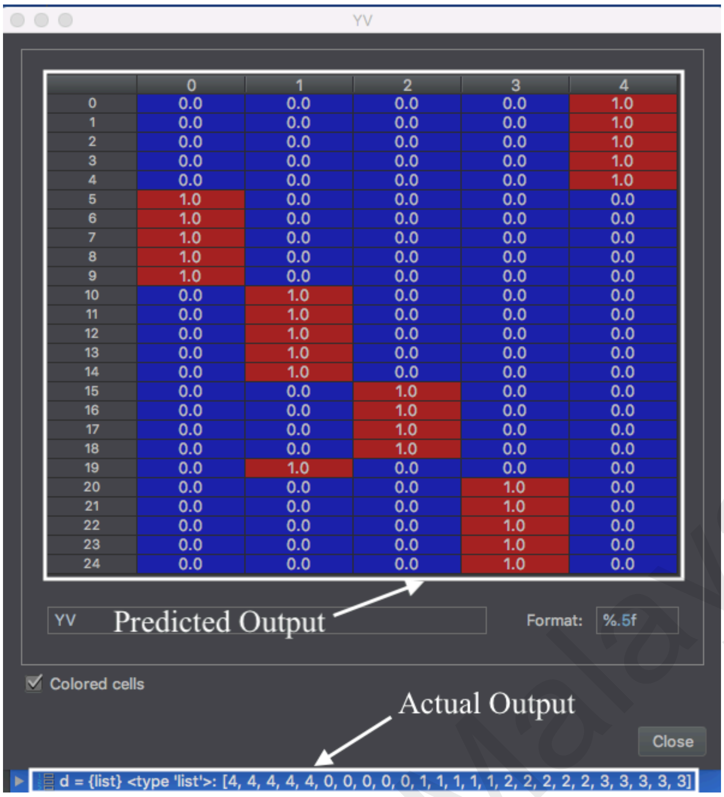

Figure 4.14: One-hot encoding results for predicted output and actual output

Table 4.4: Testing FRFs output results in form of one-hot encoded

No of Testing FRFs	Actual Output					Predicted Output				
	Damaged1	Damaged2	Damaged3	Damaged4	Undamaged	Damaged1	Damaged2	Damaged3	Damaged4	Undamaged
1	0	0	0	0	1	0	0	0	0	1
2	0	0	0	0	1	0	0	0	0	1
3	0	0	0	0	1	0	0	0	0	1
4	0	0	0	0	1	0	0	0	0	1
5	0	0	0	0	1	0	0	0	0	1
6	1	0	0	0	0	1	0	0	0	0
7	1	0	0	0	0	1	0	0	0	0
8	1	0	0	0	0	1	0	0	0	0
9	1	0	0	0	0	1	0	0	0	0
10	1	0	0	0	0	1	0	0	0	0
11	0	1	0	0	0	0	1	0	0	0
12	0	1	0	0	0	0	1	0	0	0
13	0	1	0	0	0	0	1	0	0	0
14	0	1	0	0	0	0	1	0	0	0
15	0	1	0	0	0	0	1	0	0	0
16	0	0	1	0	0	0	0	1	0	0
17	0	0	1	0	0	0	0	1	0	0
18	0	0	1	0	0	0	0	1	0	0
19	0	0	1	0	0	0	0	1	0	0
20	0	0	1	0	0	0	1	0	0	0
21	0	0	0	1	0	0	0	0	1	0
22	0	0	0	1	0	0	0	0	1	0
23	0	0	0	1	0	0	0	0	1	0
24	0	0	0	1	0	0	0	0	1	0
25	0	0	0	1	0	0	0	0	1	0

4.3: Training Samples Reduction

There are several approaches in improving the neural network performance and one of the ways is improving with data as stated in the literature review earlier. The easiest way to improve with data is by adding more data for each condition on each sensor into the training dataset and repeating the modal analysis experiment to acquire the data, also known as number of averages. Since different sensor location produces different FRF pattern output, reducing the number of sensors do not affect the performance as much as reducing number of averages. Unlike reducing the frequency range in the training FRF, if the correct mode is not selected it will lead to reduce in performance accuracy of the model. Both reduction in number of sensors and the frequency range lead to reduction in samples used to train the ANN model. Therefore, this section will discuss on the second and third objectives of this research project.

4.3.1: Reduction number of sensors

The reduction in number of sensors starts with nine (9) sensors and end with only a single sensor. First, the sensors located near the damaged points (Point 1,3,7,9 – Tyres location) were removed in order to reduce number of sensor. This is because in real case simulation, it is the most least convenient location to place a sensor. The reason sensor at point 4 and 5 were chosen because point 4 located near the side of the plate (similarly with point 6) as for point 5 it is located at the center of the plate which can relate to the vibration response for each vibration mode.

Table 4.5 shows the findings gathered from different number of sensors with different compositions (conditions x sensors x average). The table shows the performance accuracy for each composition, by evaluating the performance using cross-validation method on EMA dataset. Based on Table 4.5, the performance accuracy on EMA dataset group A,B and C decrease as the number of averages decreases. This supports the claim as the number of averages increases, the performance of ANN model will also increases.

When the number of sensors are reduced to a single sensor (Group D and E), the composition that used the lowest number of samples needed to train the ANN with 100% performance accuracy on EMA dataset for both group is the 5 x 1 x 3 composition.

Table 4.6 shows the performance accuracy for each composition, by evaluating the performance using train/test method on ISMA dataset. Based on Table 4.6, it also can be observed that the performance accuracy using ISMA dataset as a testing dataset for Group A are not as high as Group B, C, D and E. The reason behind this is the ANN was trained based on nine (9) sensors FRFs and tested with only five (5) sensors ISMA FRFs as stated earlier in the previous section (ISMA FRF Validation). The training and testing FRFs need to have equal number of sensors and sensor location in order to acquire high performance accuracy. Moreover, for Group B, C, D and E give 100% performance accuracy by using ISMA as the testing dataset. Therefore, it is possible to reduce the number of sensors to a single sensor without affecting the performance.

Lastly, the final choice for the optimized number of sensors and composition is the ones highlighted in green, with a composition of 5 x 1 x 3 for the EMA dataset and 5 x 1 x 1 for the ISMA dataset. These findings proved that it is possible to reduce the number of sensors without affecting the performance of the ANN model. The selected choice will be used in the next section whereby the number of samples are further reduced by reducing the frequency range of the FRF.

Table 4.5: Performance of the ANN based on reduction in number of sensors during stationary (EMA as testing datasets)

EMA Dataset (Training & Testing)						10-fold Cross-validation method
(Group) Number of Sensors	Sensor Point	Number of averages	Compositions (Conditions x Sensors x Averages)	Number of FRFs	Number of samples (Number of FRFs x 200)	Performance accuracy on EMA dataset (%)
(A) 9	1,2,3,4,5,6,7,8,9	5	5 x 9 x 5	225	90000	100.00%
		4	5 x 9 x 4	180	72000	100.00%
		3	5 x 9 x 3	135	54000	91.04%
		2	5 x 9 x 2	90	36000	88.84%
		1	5 x 9 x 1	45	18000	54.50%
(B) 5	2,4,5,6,8	5	5 x 5 x 5	125	50000	100.00%
		4	5 x 5 x 4	100	40000	100.00%
		3	5 x 5 x 3	75	30000	94.64%
		2	5 x 5 x 2	50	20000	86.00%
		1	5 x 5 x 1	25	10000	31.67%
(C) 4	2,4,6,8	5	5 x 4 x 5	100	40000	100.00%
		4	5 x 4 x 4	80	32000	100.00%
		3	5 x 4 x 3	60	24000	91.67%
		2	5 x 4 x 2	40	16000	100.00%
		1	5 x 4 x 1	20	8000	25.00%
(D) 1	4	5	5 x 1 x 5	25	10000	95.00%
		4	5 x 1 x 4	20	8000	100.00%
		3	5 x 1 x 3	15	6000	100.00%
		2	5 x 1 x 2	10	4000	90.00%
		1	5 x 1 x 1	5	2000	0.00%
(E) 1	5	5	5 x 1 x 5	25	10000	100.00%
		4	5 x 1 x 4	20	8000	100.00%
		3	5 x 1 x 3	15	6000	100.00%
		2	5 x 1 x 2	10	4000	100.00%
		1	5 x 1 x 1	5	2000	0.00%

Table 4.6: Performance of the ANN based on reduction in number of sensors during operation (ISMA as testing datasets)

EMA Dataset (Training)		ISMA Dataset (Testing)						Train/Test method
(Group) Number of Sensors	Number of samples	(Group) Number of Sensors	Sensor Point	Number of averages	Compositions (Conditions x Sensors x Averages)	Number of FRFs	Number of samples (Number of FRFs x 200)	Performance accuracy by using ISMA as testing dataset (%)
(A) 9	90000	(A) 5	2,4,5,6,8	1	5 x 5 x 1	25	10000	96.00%
	72000							96.00%
	54000							96.00%
	36000							92.00%
	18000							96.00%
(B) 5	50000	(B) 5						100.00%
	40000							100.00%
	30000							100.00%
	20000							96.00%
	10000							100.00%
(C) 4	40000	(C) 4	2,4,6,8		5 x 4 x 1	20	8000	100.00%
	32000							100.00%
	24000							100.00%
	16000							100.00%
	8000							100.00%
(D) 1	10000	(D) 1	4		5 x 1 x 1	5	2000	100.00%
	8000							100.00%
	6000							100.00%
	4000							100.00%
	2000							100.00%
(E) 1	10000	(E) 1	5					100.00%
	8000							100.00%
	6000							100.00%
	4000							100.00%
	2000							100.00%

4.3.2: Sensor location, frequency range and vibration mode

In this section, the main focus will be in minimizing the frequency range used in training and testing the ANN model without affecting the performance and also to study the relationship between the sensor location and the performance by selecting the correction vibration mode. The training and testing FRFs need to have equal number of total outputs/FRF because as stated earlier in the methodology the number of neurons for the ANN input layer need to be equal with the number of total outputs/FRF.

First, it is important to choose the correct frequency range based on the vibration mode. Figures 4.15 and 4.16 show two different EMA FRFs at two different sensor point (Point 4 and Point 5), focused on the 1^{st}, 2^{nd} and 3^{rd} vibration modes. It can be observed that the 3^{rd} vibration mode (Circled), sensor point 4 produced higher magnitude than sensor point 5. Thus, it is difficult to differentiate between each condition for sensor point 5. FRFs at sensor point 5 shows that the FRFs look almost identical between each condition unlike at sensor point 4. This lack of differentiation between each condition can affect the performance accuracy of the ANN model.

As for the FRF 1^{st} vibration mode shows the vibration mode at sensor point 5 is slightly higher in magnitude than at sensor point 4. This might affect the performance accuracy when the ANN model include the 1^{st} vibration mode later in reducing the frequency range. Therefore, choosing the correct vibration mode in reducing the frequency range is important to ensure that the performance accuracy of the ANN model would not get affected.

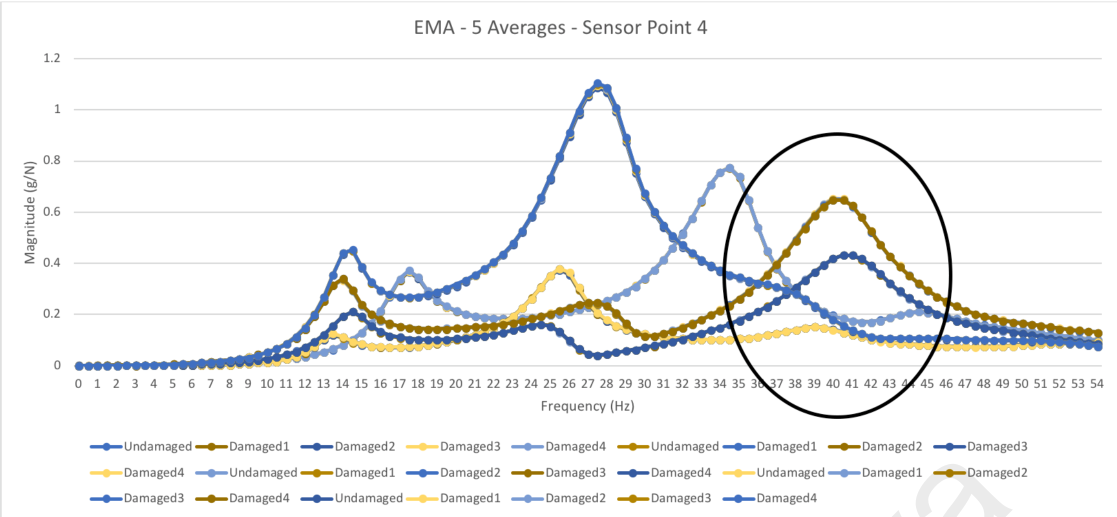

Figure 4.15: EMA FRFs at sensor point 4, circled 3rd vibration mode

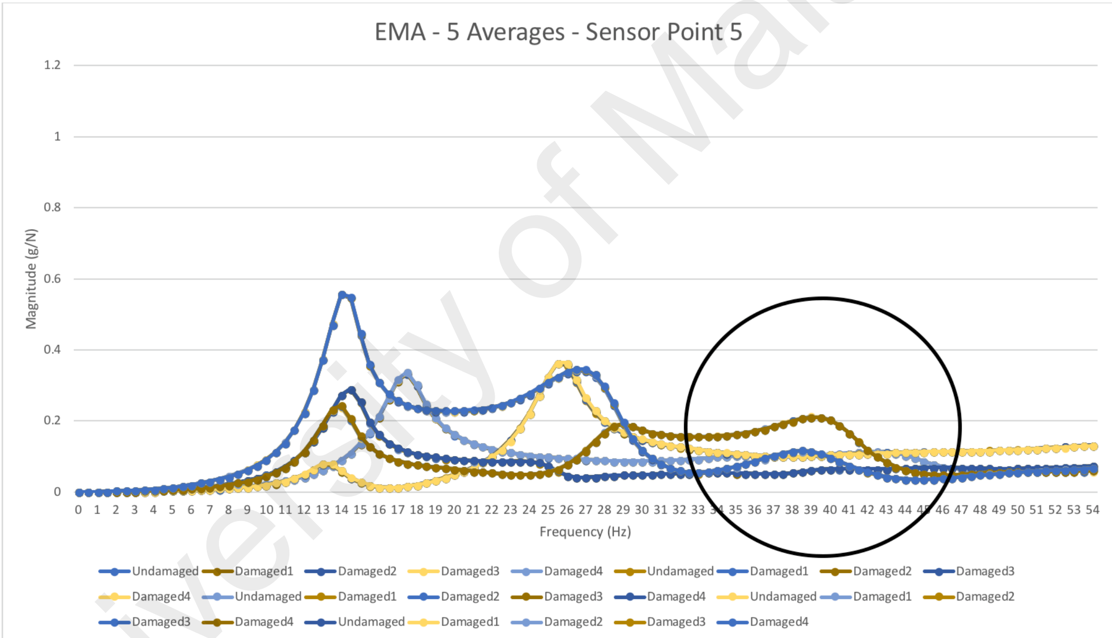

Figure 4.16: EMA FRFs at sensor point 5, circled 3rd vibration mode

Tables 4.7 and 4.8 shows the performance of the ANN based on reduction in frequency range by using 10-fold CV method on EMA dataset and Train/Test method with ISMA as testing dataset, respectively. Based on Table 4.7, it can be observed that there is a reduction in performance accuracy when the vibration mode is decreased from 5 vibration modes to only a single vibration mode. Moreover, the performance accuracy for the vibration mode 2, 3 and 3 which are highlighted in yellow, sensor point 5 has the lower performance than sensor point 4 with 70%/45% and 85%/70%, respectively. This supports the previous findings regarding the FRFs graphs in Figures 4.15 and 4.16. For the FRFs consist of 1st, 2nd and 3rd vibration modes, it can be observed that the performance sensor point 5 is higher than sensor point 4 with 100%/80%, respectively. 1st vibration mode has more dominance in differentiating the conditions which lead to increase in performance. These leave with two choices, having lesser frequency range with 85% ANN performance or more frequency range by including the 1st vibration mode with 100% ANN performance. If the 1st vibration mode is included in the training dataset, point 5 is preferably the best choice with higher performance percentage. If the 1st vibration mode is excluded from the training dataset, point 4 is preferably the best choice with lesser frequency range and training samples. Figures 4.17, 4.18, 4.19 and 4.20 show the 1st, 2nd, 3rd and 4th mode shapes using EMA, when the system was stationary. First mode shape showed all points in the simulation rig moves up and down together. This implies that first mode for the automobile simulation rig is heaving. In heaving, all the nodal points are affected therefore producing significant differentiation in magnitude for the 1st vibration mode graph as can be seen in Figures 4.15 and 4.16 for point 4 and 5 respectively. For second mode, point 1, 4 and 7 of simulation rig move up and down together while 180 degree out of phase with point 3, 6 and 9. Point 2, 5 and 8 are nodal point and shows stationary at second mode. This implies that second mode is rolling. In rolling, point 4 produced significant differentiation in magnitude than point 5 for the 2nd vibration mode in the FRF graph. For third mode, point 1, 2, 3 and 4 of simulation rig move up and down together while 180 degree out of phase with point 7, 8 and 9. Point 5 and 6 are nodal points show stationary at third mode. This implies that third mode is pitching. In pitching, it can be observed that point 5 did not produce significant differentiation in magnitude as can be seen in Figure 4.16 due to its stationary position. For forth mode, point 1 and 9 oscillate in phase with each other while point 3 and 7 oscillate in phase with each other. However, point 1 and 9 are 180 degree out of phase as compared to point 3 and 7.

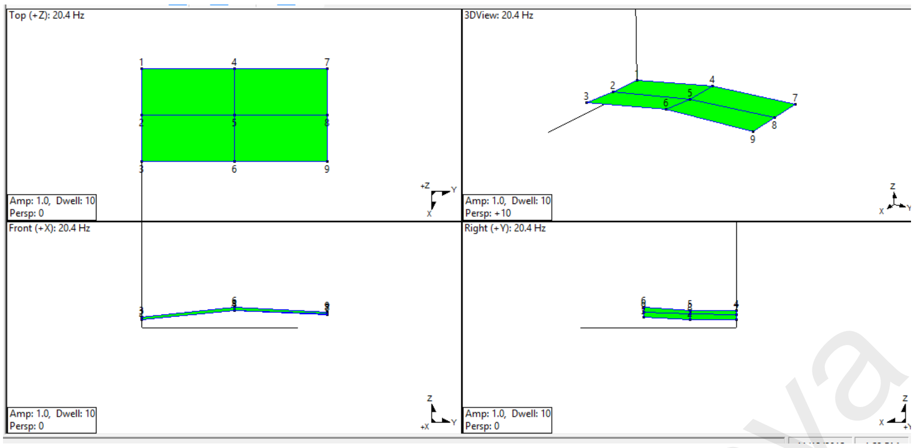

Figure 4.17: First mode shape using EMA with impact hammer

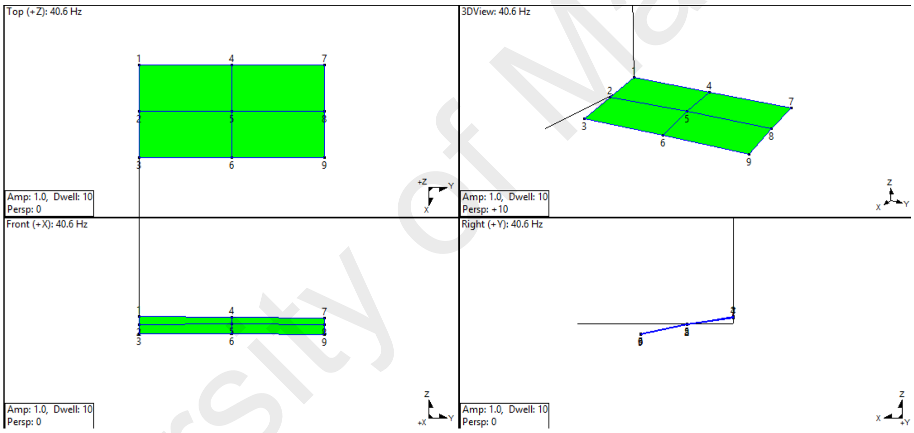

Figure 4.18: Second mode shape using EMA with impact hammer

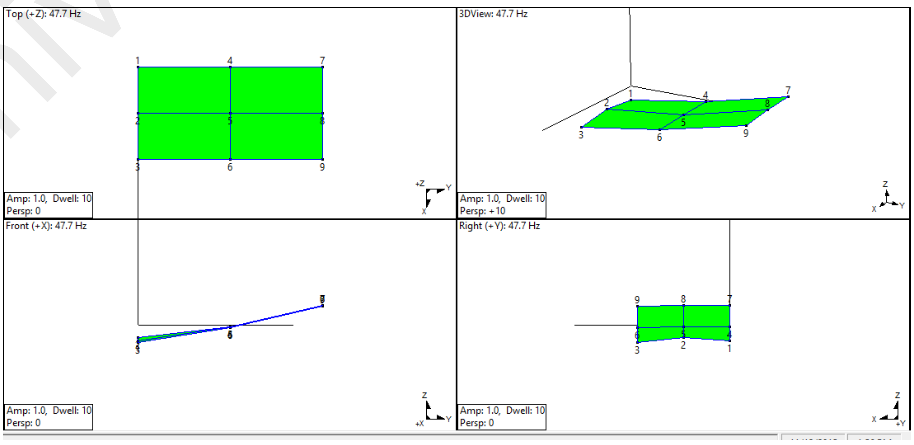

Figure 4.19: Third mode shape using EMA with impact hammer

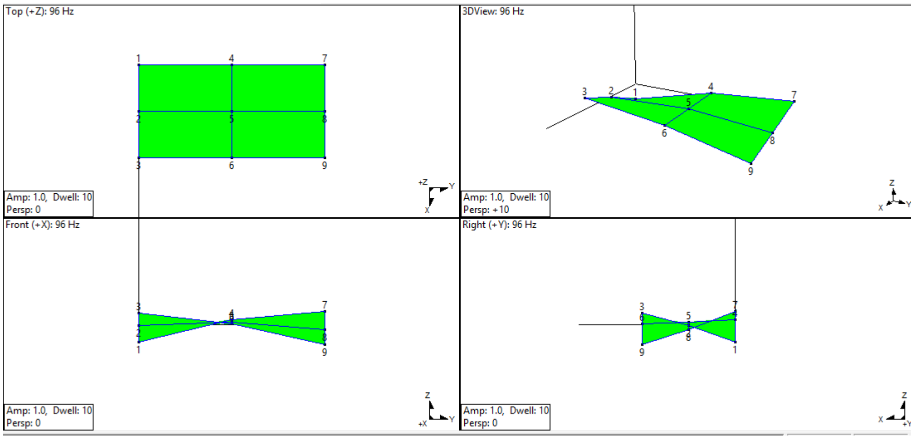

Figure 4.20:Forth mode shape using EMA with impact hammer

Based on Table 4.8, the performance accuracy for different vibration modes show consistent results between sensor point 4 and sensor point 5. The performance accuracy produced are all 100% except for the FRFs that only include a single, 3rd vibration mode.

With the overall findings, the final choice for the optimized number of sensors and frequency range used is the one highlighted in green, with a frequency range of 0Hz to 54Hz consist of 1st, 2nd and 3rd vibration modes. These findings proved that it is possible to reduce the number of sensors and frequency range by selecting the correct vibration modes without affecting the performance of the ANN model. Below is the final selection details: -

- Sensor Point 5
- Composition: 5 x 1 x 3 for EMA and 5 x 1 x 1 for ISMA
- Frequency Range: 0 Hz – 54 Hz
- Vibration modes: 1st, 2nd and 3rd
- Number of FRFs: 15 EMA FRFs and 5 ISMA FRFs
- Total number of samples: 1635 EMA samples and 545 ISMA samples
- Performance accuracy for 10-fold CV method on EMA dataset: 100%
- Performance accuracy for Train/Test method by using ISMA as testing dataset: 100%

Table 4.7: Performance of the ANN based on reduction in frequency range during stationary (EMA as testing dataset)

EMA Dataset (Training & Testing)							10-fold Cross-validation method
Sensor Point	Composition (Conditions x Sensors x Averages)	Frequency Range (Hz)	Vibration Mode	Number of FRFs	Total number of outputs/FRF	Number of samples (Number of FRFs x Total number of outputs/FRF)	Performance accuracy on EMA dataset (%)
4	5 x 1 x 3	0 - 199.5	1,2,3,4,5	15	400	6000	100%
		0 - 54	1,2,3		109	1635	80%
		20 - 54	2,3		69	1035	85%
		32 - 54	3		45	675	50%
5		0 - 199.5	1,2,3,4,5		400	6000	100%
		0 - 54	1,2,3		109	1635	100%
		20 - 54	2,3		69	1035	70%
		32 - 54	3		45	675	45%

Table 4.8: Performance of the ANN based on reduction in frequency range during operation (ISMA as testing dataset)

EMA Dataset (Training)	ISMA Dataset (Testing)							Train/Test method
Number of samples (Number of FRFs x Total number of outputs/FRF)	Sensor Point	Composition (Conditions x Sensors x Averages)	Frequency Range (Hz)	Vibration Mode	Number of FRFs	Total number of outputs/FRF	Number of samples (Number of FRFs x Total number of outputs/FRF)	Performance accuracy by using ISMA as testing dataset (%)
6000	4	5 x 1 x 1	0 - 199.5	1,2,3,4,5	5	400	2000	100%
1635			0 - 54	1,2,3		109	545	100%
1035			20 - 54	2,3		69	345	100%
675			32 - 54	3		45	225	80%
6000	5		0 - 199.5	1,2,3,4,5		400	2000	100%
1635			0 - 54	1,2,3		109	545	100%
1035			20 - 54	2,3		69	345	100%
675			32 - 54	3		45	225	80%

Chapter 5: Conclusion

5.1: Conclusions

This study managed to design a damage identification scheme using the FRF data gathered from experiment done with EMA and ISMA method with ANN. The ANN architecture used for the damage identification scheme was with only a single hidden layer consist of twenty (20) neurons. The damage identification scheme produced a 100% performance accuracy for both the CV method using EMA dataset and Train/Test method by using ISMA as the testing dataset. The ISMA FRF collected from the experiment can be consider valid and usable for the damage identification scheme. The FRF dataset that need to be used for the damage identification scheme are also interchangeable for testing and training between EMA and ISMA datasets. From the FRF graph analysis, it was found that when the structure is damaged, the FRFs graph are shifted to the left side towards lower frequency range.

Also, the number of samples used to train the ANN model managed to be reduced by reducing the number of sensors to only a single sensor from nine sensor and a frequency range consist of only three (3) vibration modes from five (5) vibration modes. The sensor point that was selected is at point 5, with a frequency range of 0 Hz – 54 Hz consist of 1st, 2nd and 3rd vibration modes. The number of FRFs used were 15 EMA FRFs and 5 ISMA FRFs with a total number of samples of 1635 and 545 for EMA and ISMA respectively. Both the CV method using EMA dataset and Train/Test method using ISMA as the testing dataset produced 100% in performance accuracy for the selected choice. This proved that is it possible to reduce the number of samples used without affecting the performance of the ANN model.

It was also found that the sensor located at point 5 consist of 2nd and 3rd vibration modes produced lower performance than the sensor located at point 4 with similar vibration modes. The FRF magnitude for sensor located at point 4, 3rd vibration mode, was higher and easy to differentiate between conditions than the sensor located at point 5, 3rd vibration mode. Thus, choosing the correct vibration mode in reducing the frequency range is important to ensure that the performance accuracy of the ANN model would not get affected. It is found that there is a correlation between the sensor location and the vibration mode.

5.2: Recommendations

Based on the methodology and findings of this study, future recommendations can be made as follow:-

- This study final selection for number of sensors and frequency range that were used to train the ANN model was tested only with five (5) ISMA samples, which provide 100% performance accuracy. Future study need to increase the number of testing samples and study the performance of the final selection.
- In this study the author only limit the number of conditions to only five (5) conditions, one (1) undamaged and four (4) damaged locations. Future recommendation would be to increase the number of conditions which simulate a real machine.
- In this study the author limits the input datasets to only a single location of impact or reference point, which is located at point 1. Future study can increase the number of reference points by creating more complex scenario and conditions.
- This study limit scope only covers up until the location of damage. Future study need to look into the damage severity and the life span of the structure.

References

A. Brandt (2011). Noise and Vibration Analysis: Signal Analysis and Experimental Procedures: Wiley.

A.G.A. Rahman, O.Z. Chao, Z. Ismail (2011). Effectiveness of Impact-Synchronous Time Averaging in determination of dynamic characteristics of a rotor dynamic system, Measurement, Vol. 44, No. 1, pp. 34-45.

A.G.A. Rahman, Z.C. Ong, Z. Ismail (2011). Enhancement of coherence functions using time signals in Modal Analysis, Measurement, Vol. 44, No. 10, pp. 2112-2123.

A.G.A. Rahman, et al. (2013). Impact-Synchronous Modal Analysis (ISMA) - An Attempt to Find an Alternative, in 5th International Operational Modal Analysis Conference: Guimarães Portugal.

A.G.A. Rahman, et al. (2014) Enhancement of Impact-synchronous Modal Analysis with number of averages, Journal of Vibration and Control, Vol. 20, No. 11, pp. 1645-1655.

Bandara, R., Chan, T., & Thambiratnam, D. (2014). Frequency response function based damage identification using principal component analysis and pattern recognition technique. Engineering Structures, 66, 116-128. doi: 10.1016/j.engstruct.2014.01.044

D. Brown, et al. (1979). Parameter estimation techniques for modal analysis, SAE Technical paper.

F1 Score. (n.d). In Wikipedia. Retrieved April 17, 2018, from https://en.wikipedia.org/wiki/F1_score.

F.V. Veen (2016). A mostly complete chart of neural networks. Retrieved from asimovinstiture.org.

Golinval, J. (2017). Damage Detection in Structures Based on Principal Component Analysis of Forced Harmonic Responses. Procedia Engineering, 199, 1912-1918. doi: 10.1016/j.proeng.2017.09.449

Haywood, J., Coverley, P., Staszewski, W., & Worden, K. (2004). An automatic impact monitor for a composite panel employing smart sensor technology. Smart materials and structures, 14(1), 265.

Hakim, S.J.S. (2006). Development and applications of artificial neural network for prediction of ultimate bearing capacity of soil and compressive strength of concrete, Master Thesis, Department of Civil Engineering, Faculty of Engineering, University Putra Malaysia, Malaysia.

Hakim, S.J.S., Noorzaei, J., Jaafar, M.S., Jameel, M. and Mohammadhassani, M. (2011). Application of artificial neural networks to predict compressive strength of high strength concrete, Int. J. Phys. Sci. (IJPS), 6(5), 975-981.

Hakim, S.J.S. and Abdul Razak, H. (2011a). Application of combined artificial neural networks and modal analysis for structural damage identification in bridge girder, Int. J. Phys. Sci. (IJPS), 6(35), 7991-8001.

Hakim, S.J.S. and Abdul Razak, H. (2011b). Damage detection of steel bridge girder using artificial neural networks, Proceedings of the 5th International Conference on Emerging Technologies in Non-Destructive Testing, 19-21 September, Ioannina, Greece

Hakim, S.J.S. and Abdul Razak, H. (2013b). Adaptive Neuro Fuzzy Inference System (ANFIS) and Artificial Neural Networks (ANNs) for structural damage identification, Struct. Eng. Mech., 45(6) 779-802.

How To Improve Deep Learning Performance. (2016, September 21). Retrieved from https://machinelearningmastery.com/improve-deep-learning-performance/

J. Brownlee (2018), Introduction to Python Deep Learning with Keras. Retrieved from https://machinelearningmastery.com/introduction-python-deep-learning-library-keras/.

J.M. Leuridan, D.L. Brown, R.J. Allemang, (1986). Time Domain Parameter-Identification Methods for Linear Modal-Analysis - a Unifying Approach, Journal of Vibration Acoustics Stress and Reliability in Design-Transactions of the Asme, Vol. 108, No. 1, pp. 1-8.

LeClerc, J., Worden, K., Staszewski, W., & Haywood, J. (2007). Impact detection in an aircraft composite panel—A neural-network approach. Journal of Sound and Vibration, 299(3), 672-682.

L. H. Cheet, O.Z. Chao (2016). Development of adaptive phase control impact device for enhancement of frequency response function in operational modal testing, Department of Mechanical Engineering.

M. Gordan, Abdul Razak, H., Z. Ismail, Z. Ibrahim. (2017). Vibration - Based Structural Damage Identification Using Data Mining. 10.13140/RG.2.2.35401.03686.

M.H. Richardson, D.L. Formenti (1982). Parameter estimation from frequency response measurements using rational fraction polynomials, in Proceedings of the 1st international modal analysis conference: Union College Schenectady, NY.

M.H. Richardson, D.L. Formenti (1985). Global curve fitting of frequency response measurements using the rational fraction polynomial method, in Proceedings of the Third International Modal Analysis Conference.

M.H. Richardson (1986). Global frequency & damping estimates from frequency response measurements, in Proceedings of the Fourth International Modal Analysis Conference.

N.-J. Jacobsen, P. Andersen, R. Brincker (2006). Using enhanced frequency domain decomposition as a robust technique to harmonic excitation in operational modal analysis, in International Conference on Noise and Vibration Engineering (ISMA), Leuven, Belgium.

O.Z. Chao (2013). Development of impact-synchronous modal analysis technique on motor-driven structure during operation, Department of Mechanical Engineering, Ph.D.

O.Z. Chao, M.A.M.A. Kor, A. Brandt (2015). Experimental Validation of Phase Synchronisation Effects in Optimising Impact-Synchronous Time Averaging, in 6th Iomac: International Operational Modal Analysis Conference Proceedings.

O.Z. Chao, et al. (2016). Assessment of the phase synchronization effect in modal testing during operation.

R.J. Allemang (1998). D.L. Brown, A unified matrix polynomial approach to modal identification, Journal of Sound and Vibration, Vol. 211, No. 3, pp. 301-322.

R. Brincker, L.M. Zhang, P. Andersen (2000). Modal identification from ambient responses using frequency domain decomposition, in Proc. of the 18th International Modal Analysis Conference (IMAC), San Antonio, Texas.

R. Brincker, L.M. Zhang, P. Andersen (2001). Modal identification of output-only systems using frequency domain decomposition, Smart Materials & Structures, Vol. 10, No. 3, pp. 441 445.

R. Brincker, L.M. Zhang, P. Andersen (2001). Modal indicators for operational modal identification, in 19th International Modal Analysis Conference (IMAC), Kissimmee, Florida.

Santos, Adam & Silva, Moisés & Sales, C.S. & Costa, J.C.W.A. & Figueiredo, Eloi. (2015). Applicability of linear and nonlinear principal component analysis for damage detection. Conference Record - IEEE Instrumentation and Measurement Technology Conference. 2015. 869-874. 10.1109/I2MTC.2015.7151383.

Suresh, S., Omkar. S.N., Ganguli. R. and Mani, V. (2004). Identification of crack location and depth in a cantilever beam using a modular neural network approach, Smart Mater. Struct., 13, 907-915.

S.J.S Hakim, H. Abdul Razak (2013). Structural damage detection of steel bridge girder using artificial neural networks and finite element models.

S.J.S Hakim, H. Abdul Razak (2014). Modal parameters based structural damage detection using artificial neural network.

SKF Condition Monitoring, I. Vibration sensors (1999). Retrieved from http://www.exvalos.cz/soubory/File/SKF/SNIMACE_VIBRACI.pdf.

Rytter, A. (1993). Vibration based inspection of civil engineering structures, PhD. Dissertation, Department of Building Technology and Structural Engineering, Aalborg University, Denmark.

Weaver Jr, W., Timoshenko, S. P., & Young, D. H. (1990). Vibration problems in engineering: John Wiley & Sons.

Worden, K., & Staszewski, W. (2000). Impact location and quantification on a composite panel using neural networks and a genetic algorithm. Strain, 36(2), 61-68.